Glutamate triggers intracellular Ca^{2+} oscillations and nitric oxide release by inducing NAADP and InsP - dependentCa^{2+} release in mouse brain endothelial cells

Estella Zuccolo[1]* | Dlzar A. Kheder[1,2]* | Dmitry Lim[3] | Angelica Perna[4] |

Francesca Di Nezza[5] | Laura Botta[1] | Giorgia Scarpellino[1] | Sharon Negri[1] |

Simona Martinotti[6] | Teresa Soda[7,8] | Greta Forcaia[10] | Laura Riboni[9] |

Elia Ranzato[6] | Giulio Sancini[10] | Luigi Ambrosone[11] | Egidio D'Angelo[8,12] |

Germano Guerra[4†] | Francesco Moccia[1†]

[1]Laboratory of General Physiology, Department of Biology and Biotechnology "Lazzaro Spallanzani," University of Pavia, Pavia, Italy

[2]Department of Biology, University of Zakho, Duhok, Kurdistan-Region of Iraq

[3]Department of Pharmaceutical Sciences, University of Eastern Piedmont "Amedeo Avogadro," Novara, Italy

[4]Department of Medicine and Health Sciences "Vincenzo Tiberio," University of Molise, Campobasso, Italy

[5]Department of Bioscience and Territory (DIBT), University of Molise, Contrada Lappone Pesche, Isernia, Italy

[6]Dipartimento di Scienze e Innovazione Tecnologica (DiSIT), University of Piemonte Orientale, Alessandria, Italy

[7]Museo Storico della Fisica e Centro Studi e Ricerche Enrico Fermi, Rome, Italy

[8]Department of Brain and Behavioral Sciences, University of Pavia, Pavia, Italy

[9]Department of Medical Biotechnology and Translational Medicine, LITA-Segrate, University of Milan, Segrate, Milan, Italy

[10]Department of Medicine and Surgery, University of Milano-Bicocca, Monza, Italy

[11]Department of Medicine and Health Sciences "Vincenzo Tiberio," Centre of Nanomedicine, University of Molise, Campobasso, Italy

[12]Brain Connectivity Center, C. Mondino National Neurological Institute, Pavia, Italy

The neurotransmitter glutamate increases cerebral blood flow by activating postsynaptic neurons and presynaptic glial cells within the neurovascular unit. Glutamate does so by causing an increase in intracellular Ca2+ concentration ([Ca2+]i) in the target cells, which activates the Ca2+/Calmodulin-dependent nitric oxide (NO) synthase to release NO. It is unclear whether brain endothelial cells also sense glutamate through an elevation in [Ca2+]i and NO production. The current study assessed whether and how glutamate drives Ca2+dependent NO release in bEND5 cells, an established model of brain endothelial cells. We found that glutamate induced a dose-dependent oscillatory increase in [Ca2+]i, which was maximally activated at 200 μM and inhibited by α-methyl-4-carboxyphenylglycine, a selective blocker of Group 1 metabotropic glutamate receptors. Glutamate-induced intracellular Ca2+ oscillations were triggered by rhythmic endogenous Ca2+ mobilization and maintained over time by extracellular Ca2+ entry. Pharmacological manipulation revealed that glutamate-induced endogenous Ca2+ release was mediated by InsP3-sensitive receptors and nicotinic acid adenine dinucleotide phosphate

(NAADP) gated two-pore channel 1. Constitutive store-operated Ca^{2+} entry mediated Ca^{2+} entry during ongoing Ca^{2+} oscillations. Finally, glutamate evoked a robust, although delayed increase in NO levels, which was blocked by pharmacologically inhibition of the accompanying intracellular Ca^{2+} signals. Of note, glutamate induced Ca^{2+}-dependent NO release also in hCMEC/D3 cells, an established model of human brain microvascular endothelial cells. This investigation demonstrates for the first time that metabotropic glutamate-induced intracellular Ca^{2+} oscillations and NO release have the potential to impact on neurovascular coupling in the brain.

INTRODUCTION

Functional hyperemia is the mechanism by which an increase in neuronal activity leads to a local elevation in cerebral blood flow (CBF) to adjust oxygen and glucose delivery to the requirements of the activated brain structures. The complex interplay between neurons, astrocytes and vascular cells (endothelial cells, vascular smooth muscle cells and pericytes) that ensures adequate blood flow to firing neurons has been termed neurovascular coupling (NVC; Attwell et al., 2010; Kisler, Nelson, Montagne, & Zlokovic, 2017). A wealth of studies have been devoted to unravel the signal transduction pathways at work within this "neuronal-astrocyticvascular" tripartite unit, also known as the neurovascular unit (NVU; Attwell et al., 2010; Hamel, 2006; Hillman, 2014; Kisler et al., 2017; Lecrux & Hamel, 2016). Although other neurotransmitters may play a role (Hamel, 2006; Lecrux & Hamel, 2016), the excitatory amino acid glutamate represents the most common trigger for NVC (Attwell et al., 2010; Kisler et al., 2017). Synaptically released glutamate may initiate direct neuronal-to-vascular communication by activating neuronal N-methyl D-aspartate receptors (NMDARs). NMDARsmediated extracellular Ca^{2+} entry leads to the recruitment of the Ca^{2+}-dependent neuronal nitric oxide (NO) synthase and, thereafter, causes NO release. NO, in turn, induces vasodilation in both cerebellar (Lauritzen, Mathiesen, Schaefer, & Thomsen, 2012; Mapelli et al., 2017) and hippocampal microvasculature (Lourenco, Ledo, Barbosa, & Laranjinha, 2017), while it plays a permissive role in arachidonic acid (AA) metabolite-induced vasodilation in the cortex by suppressing the synthesis of the vasoconstricting, 20-hydroxyeicosatetraenoic acid (20-HETE; Attwell et al., 2010). This last mechanism requires astrocytes to serve as functional mediators of the exchange of vasoactive signals between neurons and cerebral microvessels. Accordingly, the synaptic release of glutamate could also activate the astrocyte $G_{q/11}$ coupled Group I metabotropic glutamate receptors (mGluRs), mGluR1 and mGluR5, resulting in phospholipase Cβ (PLCβ) activation, inositol-1,4,5-trisphosphate ($InsP_3$) synthesis and endoplasmic reticulum (ER)-dependent intracellular Ca^{2+} release (Attwell et al., 2010; Lim et al., 2013; Mishra, 2017). Glutamate-induced intracellular Ca^{2+} waves could travel from the soma to astrocyte endfeet, which wrap around cerebral

microvessels and respond to the incoming Ca^{2+} signal by synthesizing the vasorelaxing AA metabolites, prostaglandin E2 (PGE2) and epoxyeicosatrienoic acids (EETs). Furthermore, some AA can be released onto vascular smooth cells, where it is converted into 20-HETE by the NO-sensitive enzyme CYP4A (Attwell et al., 2010). Therefore, glutamate-induced NO release is required to promote PGE2- and EET-dependent functional hyperemia (Attwell et al., 2010; Hall et al., 2014). The role of astrocytes in mediating NVC has, however, been questioned by the recent finding that adult mouse astrocytes lack mGluR1 and mGluR5 (Calcinaghi et al., 2011; Sun et al., 2013). Nevertheless, the pharmacological blockade of Group I mGluRs attenuates the evoked CBF response in adult rodent somatosensory cortex (Lecrux et al., 2011; Shi et al., 2008; Zonta et al., 2003). Surprisingly, it is still unclear whether endothelial signaling actively contributes to NVC (Andresen, Shafi, & Bryan, 2006; B. R. Chen, Kozberg, Bouchard, Shaik, & Hillman, 2014; Guerra et al., 2018; Hillman, 2014), despite the fact that vascular endothelium has long been known to finely tune blood flow in peripheral vasculature (Behringer, 2017; Duncker & Bache, 2008). Recent studies revealed that glutamate may stimulate NMDARs to engage in the endothelial NO synthase (eNOS; LeMaistre et al., 2012; Stobart, Lu, Anderson, Mori, & Anderson, 2013) and that Group I mGluRs are largely expressed in brain–brain barrier (BBB; Beard, Reynolds, & Bearden, 2012; Collard et al., 2002; Gillard, Tzaferis, Tsui, & Kingston, 2003; Lv et al., 2016). It is, however, still unknown whether the metabotropic activity of glutamate is able to induce intracellular Ca^{2+} signals and NO release in brain endothelial cells.

Brain microvascular endothelial cells are able to sense a plethora of extracellular transmitters and growth factors, which bind to their selective $G_{q/11}$-coupled metabotropic receptors and, thereafter, trigger intracellular Ca^{2+} oscillations to enlist specific downstream Ca^{2+}dependent decoders (De Bock et al., 2013; Guerra et al., 2018). For instance, bradykinin-induced repetitive Ca^{2+} spikes increase the BBB permeability in rat brain microvascular endothelial cells (De Bock et al., 2011), whereas the cerebral spinal fluid leaking onto human cerebral endothelial cells after subarachnoid hemorrhage use an oscillatory Ca^{2+} signal to stimulate nuclear factor (NF)-kappaB (NF-κB)-dependent gene expression (Scharbrodt et al., 2009). We have recently shown that acetylcholine induces intracellular Ca^{2+} oscillations to support NO release in bEND5 cells, an established model of mouse brain microvascular endothelial cells (Zuccolo et al., 2017). Acetylcholineinduced intracellular Ca^{2+} oscillations are generated by the rhythmic inositol-1,4,5-trisphosphate ($InsP_3$)-dependent Ca^{2+} discharge from the ER, whereas ryanodine receptors (RyRs) are absent in this cell line. Store-operated Ca^{2+} entry (SOCE), which is gated by depletion of the ER Ca^{2+} store (Moccia & Guerra, 2016), is constitutively activated in bEND5 cells to refill the ER Ca^{2+} pool and is further activated by acetylcholine to maintain Ca^{2+} oscillations over time (Zuccolo et al., 2017). A thorough transcriptomic analysis confirmed that SOCE is the major Ca^{2+} entry pathway and is mediated by Stim1, Stim2, and Orai2 in bEND5 cells, whereas canonical transient receptor potential channels are largely absent and, therefore, do not contribute to agonist-evoked Ca^{2+} signals (Di & Malik, 2010; Moccia, Lucariello, & Guerra, 2018). Conversely, it is still unclear whether bEND5 cells dispose of an endolysosomal (EL) Ca^{2+} store, as recently shown in vascular endothelial cells (Brailoiu et al., 2010; Favia et al., 2014) and endothelial colony forming cells (Di Nezza

et al., 2017; Zuccolo, Dragoni et al., 2016). EL Ca^{2+} is mobilized by the newly discovered Ca^{2+}-releasing second messenger, nicotinic acid adenine dinucleotide phosphate (NAADP), which binds to and gates two-pore channels 1 and 2 (TPC1–2; Guse, 2012; Patel, 2015). Of note, NAADP triggers the Ca^{2+} response to glutamate in rat hippocampal neurons and astrocytes (Pandey et al., 2009) and in SHSY5Y neuroblastoma cells (Pereira et al., 2017).

The present investigation sought to assess whether glutamate triggered intracellular Ca^{2+} oscillations and NO release in bEND5 cells. We found that glutamate evoked a dose-dependent oscillatory increase in $[Ca^{2+}]_i$ which was inhibited by (RS)-α-methyl-4-carboxyphenylglycine (MCPG), a selective antagonist of Group I mGluRs (Mapelli et al., 2017). Pharmacological manipulation revealed that glutamate-induced intracellular Ca^{2+} oscillations were supported by $InsP_3$-dependent ER Ca^{2+} release and by NAADP-induced EL Ca^{2+} mobilization. Glutamate was not able to trigger extracellular Ca^{2+} entry, but the oscillatory signal was maintained over time by constitutive SOCE. Finally, glutamate-induced intracellular Ca^{2+} oscillations led to robust, although delayed, NO release in bEND5 cells. Of note, glutamate induced Ca^{2+}-dependent NO production also in hCMEC/D3 cells, which represent an established model of human brain microvascular endothelial cells. These data show for the first time that synaptically released glutamate has the potential to trigger and/or prolong the hemodynamic response by stimulating mGluRs located on nearby microvascular endothelial cells.

1 | MATERIALS AND METHODS

1.1 | Cell culture

Mouse endothelial cell bEND5 cells were used to investigate the Ca^{2+} and NO response to glutamate in mouse brain microvascular endothelial cells. The bEND5 cell line (American Type Culture Collection, Manassas, VA) is an immortalized mouse cell line from brain capillary endothelial cells. Cells were grown in Dulbecco modified Eagle medium (Gibco Invitrogen, Carlsbad, CA) supplemented with 10% fetal calf serum, 4 mmol/L ʟ-glutamine, 1 mmol/L sodium pyruvate, 50 units/ml penicillin, and 50 mg/ml streptomycin, 1% minimal essential medium nonessential amino acids exactly, as originally described previously (Reiss, Hoch, Deutsch, & Engelhardt, 1998). Cells were cultured in a humidified cell culture incubator at 37°C and an atmosphere of 5% CO_2/95% air. The bEND5 cells used in this study were passaged between 17 and 21 times.

Human brain endothelial cells (hCMEC/D3) were obtained from Institut National de la Santé et de la Recherche Médicale (Paris, France). hCMEC/D3 cells cultured between passage 25 and 35 were used. As described in (Salvati et al., 2013; Zuccolo et al., 2017), the cells were seeded at a concentration of 27,000 cells/cm^2 and grown in tissue culture flasks coated with 0.1 mg/ml rat tail collagen type 1, in the following medium: Endothelial growth basal medium (EBM-2) (Lonza, Basel, Switzerland) supplemented with 5% fetal bovine serum, 1% Penicillin–Streptomycin, 1.4 μM hydrocortisone, 5 μg/ml ascorbic acid, 1 of 100 chemically defined lipid concentrate (Invitrogen, Milan, Italy), 10 mM 4-(2-Hydroxyethyl)piperazine-1-ethanesulfonic acid, N-(2-

Hydroxyethyl)piperazine-N'-(2-ethanesulfonic acid) (HEPES), and 1 ng/ml basic FGF. The cells were cultured at 37°C, 5% CO_2 saturated humidity.

1.1.1 | Solutions

Physiological salt solution (PSS) had the following composition (in mM): 150 NaCl, 6 KCl, 1.5 $CaCl_2$, 1 $MgCl_2$, 10 Glucose, and 10 HEPES. In Ca^{2+}-free solution (0Ca^{2+}), Ca^{2+} was substituted with 2 mM NaCl, and 0.5 mM EGTA was added. Solutions were titrated to pH 7.4 with NaOH. In Mn^{2+}-quenching experiments, 200 μM $MnCl_2$ was added to the 0Ca^{2+} external solution devoid of EGTA. The osmolality of PSS as measured with an osmometer (Wescor 5500, Logan, UT) was 338 mmol/kg.

1.1.2 | [Ca^{2+}]$_i$ measurements

We used the Ca^{2+} imaging set-up that we have described elsewhere (Dragoni, Guerra et al., 2015; Zuccolo et al., 2017). bEND5 cells were loaded with 4 μM Fura-2 acetoxymethyl ester (Fura-2/AM; 1 mM stock in dimethyl sulfoxide) in PSS for 30 min at room temperature. After washing in PSS, the coverslip was fixed to the bottom of a Petri dish and the cells observed by an upright epifluorescence Axiolab microscope (Carl Zeiss, Oberkochen, Germany), usually equipped with a Zeiss 40× Achroplan objective (water immersion, 2.0-mm working distance, 0.9 numerical aperture). The cells were excited alternately at 340 and 380 nm, and the emitted light was detected at 510 nm. A first neutral density filter (1 or 0.3 optical density) reduced the overall intensity of the excitation light and a second neutral density filter (optical density = 0.3) was coupled to the 380-nm filter to approach the intensity of the 340-nm light. A round diaphragm was used to increase the contrast. The excitation filters were mounted on a filter wheel (Lambda 10, Sutter Instrument, Novato, CA). Custom software, working in the LINUX environment, was used to drive the camera (Extended-ISIS Camera; Photonic Science, Millham, UK) and the filter wheel, and to measure and plot on-line the fluorescence from 20 to 45 rectangular "regions of interest" (ROI) enclosing 30–45 single cells. Each ROI was identified by a number. Adjacent ROIs never superimposed. [Ca^{2+}]$_i$ was monitored by measuring, for each ROI, the ratio of the mean fluorescence emitted at 510 nm when exciting alternatively at 340 and 380 nm

[ratio (F_{340}/F_{380})]. An increase in [Ca^{2+}]$_i$ causes an increase in the ratio [27]. Ratio measurements were performed and plotted on-line every 3 s. The experiments were performed at room temperature (22°C).

   Mn^{2+} has been shown to quench Fura-2 fluorescence. Because Mn^{2+} and Ca^{2+} share common entry pathways in the plasma membrane, Fura-2 quenching by Mn^{2+} is regarded as an index of divalent cation influx (Hallam, Jacob, & Merritt, 1988). Experiments were carried out at the 360 nm wavelength, the isosbestic wavelength for Fura-2, and in Ca^{2+}-free medium supplemented with 0.5 mM EGTA, as previously described (Moccia et al., 2002; Zuccolo, Bottino et al., 2016). This avoids Ca^{2+} competition for Mn^{2+} entry and therefore enhances Mn^{2+} quenching.

NO was measured as described in (Zuccolo, Dragoni et al., 2016) and (Zuccolo et al., 2017). Briefly, bEND5 cells were loaded with the membrane-permeable NO-sensitive dye 4-amino-5-methylamino2',7'-difluorofluorescein (DAF-FM) diacetate (10 μM) for 60 min at room temperature and washed in PSS for further 1 hr. DAF-FM fluorescence was measured by using the same equipment described for Ca^{2+} recordings but with a different filter set, that is excitation at 480 nm and emission at 535 nm wavelength (emission intensity was shortly termed "NO_i"). The changes in DAF-FM fluorescence induced by Ach were recorded and plotted on-line every 5 s. Again, off-line analysis was performed by using custom-made macros developed by Microsoft Office Excel software. The experiments were performed at room temperature (22°C).

1.1.3 | Quantitative RT-PCR

Total mRNA was extracted from approximately 2.0×10^6 cells using TRIzol Lysis Reagent (Invitrogen) and retrotranscribed to cDNA using ImProm-II RT system (Promega, Milan, Italy). Real-time polymerase chain reaction (RT-PCR) was performed using iTaq qPCR master mix according to manufacturer's instructions (Bio-Rad, Segrate, Italy) on a SFX96 realtime system (Bio-Rad). Raw qPCR expression data were normalized to S18 ribosomal subunit. Oligonucleotide primers were from Sigma and are as follows (from 5' to 3'): S18 (NM_011296): forward, TGCGAGTACT CAACACCAACA; reverse, CTGCTTTCCTCAACACCACA; Tpcn1 (NM_145853.2): forward, TTTAGATGACGATGTGCCGC; reverse, CTGGGAGTTGTGGATGCTGT; Tpcn2 (NM_146206.4): forward, TGTGGTGGACTGGATCGTTT; reverse, CCACCGTATACACTTCAGGGT. Data are expressed as ΔC(t) of Tpcn/S18 difference ± standard deviation from three independent cultures each run in triplicate.

1.1.4 | Preparation of NAADP-containing liposomes

NAADP-containing liposomes were prepared from lecithin by a thin film hydration method, as recently shown in (Di Nezza et al., 2017). A thin film was formed by dissolving the lecithin in chloroform/ methanol solution (2:1, v/v) in a round bottom flask and after the removal of the solvent under vacuum condition at room temperature, which ensured complete removal of the solvents. The film was then hydrated with PBS buffer (10 mM, pH 7.4) to make 20 ml of lipid coarse dispersion. Liposomes were prepared by adding cholesterol in an 89:20 lecithin:cholesterol molar ratio, codissolved in chloroform and then dried. The dried film from a flask was suspended in 4 ml of rehydration solution. The resulting liposomal dispersion was sonicated (Bufalo, Di Nezza, Cimino, Cuomo, & Ambrosone, 2017) for 3 min (Ultrasound Homogenizer-Biologics, Teltow, Germany) and extruded 21 times with a 100-nm filter. Finally, the mixture was dialyzed in PBS bulk for 24 hr with three bulk changes. Properties of liposomes were modulated by varying the rehydration solution composition. Liposomes were prepared from PBS solution containing only 70 g of NAADP. NAADP was diluted at 1:20, as shown elsewhere (Di Nezza et al., 2017).

1.1.5 | Statistics

All the data have been collected from bEND5 cells deriving from at least three coverslips from three independent experiments. The amplitude of Ca^{2+} release in response to glutamate (first spike) and NAADP-containing liposomes was measured as the difference between the ratio at the peak of intracellular Ca^{2+} mobilization and the mean ratio of 1-min baseline before the peak. The rate of Mn^{2+} influx was evaluated by measuring the slope of the fluorescence intensity curve at 400 s after Mn^{2+} addition (Zuccolo, Bottino et al., 2016). The amplitude of NO release in response to glutamate was measured as the difference between the peak DAF fluorescence and the average of 1-min baseline before the peak. Pooled data are given as average ± standard error (SE) and statistical significance ($p < 0.05$) was evaluated by the Student t test for unpaired observations. Data relative to both Ca^{2+} and NO signals and to Mn^{2+} influx rate are presented as average ± SE, whereas the number of cells analyzed is indicated in the corresponding bar histograms.

1.1.6 | Chemicals

Fura-2/AM and DAF-FM were obtained from molecular probes (Molecular Probes Europe BV, Leiden, The Netherlands). MCPG was purchased from ABCAM (Cambridge, UK). All other chemicals were obtained from Sigma Chemical Co. (St. Louis, MO).

2 | RESULTS

2.1 | Glutamate induces intracellular Ca^{2+} oscillations in bEND5 cells

To assess whether glutamate induces intracellular Ca^{2+} activity in bEND5 cells, cells were loaded with the Ca^{2+}-sensitive fluorochrome, Fura-2/AM, as shown elsewhere (Zuccolo et al., 2017). In the absence of extracellular stimulation, we detected spontaneous Ca^{2+} spikes arising in a fraction (≈30%) of cells that were therefore discarded from subsequent analysis. When glutamate was administrated to quiescent cells, it caused a dose-dependent oscillatory increase in $[Ca^{2+}]_i$ (Figure 1). The spiking Ca^{2+} response arose at 50 μM and achieved a peak at 200 μM; accordingly, the percentage of responding cells (Figure 2a), the amplitude of the first Ca^{2+} transient (Figure 2b), the number of Ca^{2+} spikes/30 min (Figure 2c) and the frequency of the Ca^{2+} train (Figure 2d) reached their highest value at this dose, and decreased by further increasing glutamate concentration to 300 μM. Therefore, 200 μM glutamate was used throughout the remainder of our investigation. Removal of glutamate from the perfusate caused the reversible interruption of the ongoing oscillatory signal (Figure 3a). Moreover, glutamate-induced intracellular Ca^{2+} oscillations were abolished by the broad-spectrum mGluR antagonist, MCPG (150 μM, 10 min; Figure 3b,c), in agreement with mGluR expression in the BBB (Beard et al., 2012; Collard et al., 2002; Gillard et al., 2003; Lv et al., 2016). Taken together, these findings provide the first evidence that glutamate induces metabotropic intracellular Ca^{2+} oscillations in mouse brain microvascular endothelial cells.

2.2 | Glutamate-induced intracellular Ca^{2+} oscillations require both intracellular Ca^{2+} release and extracellular Ca^{2+} entry

Our previous investigation revealed that intracellular Ca^{2+} signals in bEND5 cells may involve ER-dependent Ca^{2+} mobilization through $InsP_3$ receptors ($InsP_3Rs$) and SOCE (Zuccolo et al., 2017). Therefore, we first challenged the cells with glutamate (200 µM) in the absence of extracellular Ca^{2+} ($0Ca^{2+}$) to assess the relative contribution of endogenous Ca^{2+} release and Ca^{2+} entry to the evoked response. Glutamate still induced repetitive Ca^{2+} spikes under $0Ca^{2+}$ conditions, but these Ca^{2+} oscillations rapidly run down (Figure 4a,d) and resumed only on Ca^{2+} restitution to the bath (Figure 4a). The amplitude of the first Ca^{2+} spike was not different in the presence and absence of external Ca^{2+} (Figure 4b, c), thus suggesting that Ca^{2+} entry is not necessary to initiate the oscillations, but is strictly required to maintain them over time (Bird & Putney, 2005; Dragoni et al., 2011). Consistent with these data, removal of extracellular Ca^{2+} during ongoing oscillations abolished the spikes and returned $[Ca^{2+}]_i$ to resting levels (Figure 4b). Of note, the Ca^{2+} train did not immediately cease under $0Ca^{2+}$ conditions, but persisted for 1–2 spikes, and quickly recovered when Ca^{2+} was reapplied to extracellular saline (Figure 4a). Overall, these results indicate that glutamate-induced intracellular Ca^{2+} oscillations are shaped by the rhythmical mobilization of the intracellular Ca^{2+} reservoir and sustained by extracellular Ca^{2+} entry.

2.3 | Glutamate-induced intracellular Ca^{2+} oscillations require $InsP_3$-sensitive Ca^{2+} release from the ER

As mentioned earlier, the ER represents the main intracellular Ca^{2+}

store in bEND5 cells and delivers periodic Ca^{2+} spikes in response to extracellular stimulation through $InsP_3$ receptors ($InsP_3Rs$; Zuccolo et al., 2017). To assess whether $InsP_3$ also underlines the spiking response to glutamate, we preincubated the cells with U73122 (10 μM, 30 min), an aminosteroid PLCβ antagonist (Dragoni, Reforgiato et al., 2015). U73122 suppressed glutamate-induced intracellular Ca^{2+} spikes (Figure 5a,d), whereas its inactive analog, U73343 (10 μM, 30 min), had no effect (Figure 5a,d). Subsequently, we preincubated the cells with 2-aminoethoxydiphenylborate (2-APB; 50 μM, 30 min), which selectively inhibits $InsP_3Rs$ in the absence of extracellular Ca^{2+} ($0Ca^{2+}$; Moccia et al., 2016; Potenza et al., 2014). As shown in Figure 5a and summarized in Figure 5d, 2-APB prevented the initiation of glutamate-induced intracellular Ca^{2+} oscillations under $0Ca^{2+}$ conditions. Therefore, $InsP_3$ plays a key role in the generation of repetitive Ca^{2+} transients. To further confirm this hypothesis, we challenged the cells with cyclopiazonic acid (CPA; 10 μM), which selectively blocks Sarco-ER Ca^{2+}-ATPase (SERCA) activity, thereby preventing ER Ca^{2+} refilling. CPA was added in the absence of extracellular Ca^{2+} ($0Ca^{2+}$) and caused a prompt increase in $[Ca^{2+}]_i$ which was due to intraluminal Ca^{2+} leaking out from the ER and accumulating within the cytosol before being removed by Ca^{2+} extrusion systems (J. B. Chen et al., 2010; Sanchez-Hernandez et al., 2010). The subsequent addition of glutamate did not cause any detectable Ca^{2+} signal (Figure 5b,d), in agreement with the role played by the ER in supporting the periodic Ca^{2+} release. According to this model, after each Ca^{2+} spike, Ca^{2+} must be sequestered back by SERCA to allow the ER to continue releasing Ca^{2+} and support the intracellular Ca^{2+} waves. If this hypothesis was true, the pharmacological blockade of SERCA should suppress the Ca^{2+} spikes as the ER can no longer be replenished. Consistently, the application of CPA during

ongoing oscillations caused the expected increase in $[Ca^{2+}]_i$, followed by complete abolition of glutamate-induced intracellular Ca^{2+} spikes (Figure 5c). The $[Ca^{2+}]_i$, however, decayed to a plateau level which was indicative of SOCE activation (Dai, Kuo, Leo, van Breemen, & Lee, 2006; Syyong et al., 2009; Zuccolo et al., 2017; Figure 5c). Therefore, these data strongly support the hypothesis that $InsP_3Rs$ mediate the periodic release of ER Ca^{2+} in response to glutamate stimulation in bEND5 cells.

2.4 | Glutamate-induced intracellular Ca^{2+} oscillations require NAADP-sensitive Ca^{2+} release from the EL Ca^{2+} stores

Recent studies demonstrated that endothelial cells are endowed with an additional intracellular Ca^{2+} reservoir, which comprises endosomes and lysosomes, collectively known as acidic Ca^{2+} stores, and is targeted by NAADP (Di Nezza et al., 2017; Favia et al., 2014; Morgan, Platt, Lloyd-Evans, & Galione, 2011; Patel & Docampo, 2010; Zuccolo, Dragoni et al., 2016). NAADP, in turn, triggers Ca^{2+} release from acidic organelles by gating TPC1 and TPC2 through the interposition of an NAADP-binding protein, of which two isoforms exist (Guse, 2012). Of note, glutamate-induced increase in $[Ca^{2+}]_i$ is triggered by NAADP-sensitive acidic Ca^{2+} stores in mouse hippocampal neurons and

glia (Pandey et al., 2009) and in SHSY5Y neuroblastoma cells (Pereira et al., 2017). We used the liposome technique to stimulate bEND5 cells with the cell membrane-impermeable NAADP, as recently shown (Di Nezza et al., 2017). Liposomal application of NAADP, which was delivered in the absence of external Ca^{2+} ($0Ca^{2+}$) to prevent extracellular Ca^{2+} entry, caused a robust increase in $[Ca^{2+}]_i$ (Figure 6a). NAADPinduced Ca^{2+} release was blocked by NED-19 (10 µM, 30 min), a selective TPC antagonist (Figure 6a; Di Nezza et al., 2017; Pitt, Reilly-O'Donnell, & Sitsapesan, 2016). We further probed the effect of nigericin, a protonophore that depletes the acidic Ca^{2+} pool by collapsing the H^+ gradient across lysosomal membranes, thereby abrogating the driving force that sustains the activity of the Ca^{2+}/H^+ exchanger which refills acidic organelles with Ca^{2+} (Gambara et al., 2008; Melchionda, Pittman, Mayor, & Patel, 2016; Morgan et al., 2011; Ronco et al., 2015). Nigericin (50 µM) caused a slow, but significant elevation in $[Ca^{2+}]_i$ that prevented the subsequent Ca^{2+} response to NAADP (Figure 6b). These results are summarized in Figure 6c and demonstrate that an acidic Ca^{2+} store targeted by NAADP is present in bEND5 cells. We then exploited quantitative RT-PCR to demonstrate that both TPC1 and TPC2 are present in bEND5 cells, their expression levels being TPC1»TPC2 (Figure 6d). Subsequently, we found that glutamateinduced intracellular Ca^{2+} oscillations were abolished by Ned-19 (10 µM, 30 min; Figure 7a,b) or nigericin (50 µM; Figure 7b,c). These recordings were carried out under $0Ca^{2+}$ conditions because the initiation of the spiking response to glutamate does not require extracellular Ca^{2+} entry. Altogether, these data clearly show that NAADP-sensitive acidic Ca^{2+} stores are involved in the generation of the   rhythmical   ER Ca^{2+} discharge induced by glutamate.

2.5 | Glutamate-induced intracellular Ca^{2+} oscillations are maintained by constitutive store-operated Ca^{2+} entry

The results described in Figure 3a,d demonstrate that extracellular Ca^{2+} entry is necessary to maintain the oscillatory Ca^{2+} response to glutamate over time. SOCE represents the main pathway for agonist-induced Ca^{2+} entry in bEND5 cells, but is also heavily activated in the absence of extracellular stimulation to replenish the ER Ca^{2+} content (Zuccolo et al., 2017). Therefore, to evaluate whether SOCE is the Ca^{2+}-permeable route recruited by glutamate to sustain the intracellular Ca^{2+} oscillations, we could not preincubate the cells with any SOCE inhibitor. As widely explained in (Zuccolo, Bottino et al., 2016; Zuccolo et al., 2017), preincubation with SOCE inhibitors leads to the depletion of the ER Ca^{2+} store and prevents the onset of the Ca^{2+}-dependent response to any extracellular stimulus. To address the role of SOCE in glutamate-induced intracellular Ca^{2+} oscillations, we turned to the Mn^{2+}-quenching technique, which consists in replacing extracellular Ca^{2+} with Mn^{2+} and monitoring the consequent drop in Fura-2 fluorescence (see Section 2). Mn^{2+} is able to flow through most Ca^{2+}-permeable channels on the plasma membrane, including Orai channels (Feng et al., 2010; Zuccolo, Bottino et al., 2016), and thereafter binds to Fura-2, causing an almost linear reduction in its fluorescence signal which is indicative of Ca^{2+} entry (Jacob, 1990; Moccia et al., 2002). As expected (Zuccolo et al., 2017), we observed a clear decay in Fura-2 fluorescence on substitution of extracellular Ca^{2+} with Mn^{2+} in bEND5 cells (Figure 8a). We recently found that this constitutive Ca^{2+} entry was sensitive to the selective Orai inhibitors, Pyr6 and 10 µM La^{3+}, being, therefore, attributable to a SOCE pathway

activated under resting conditions. Glutamate, however, was not able to enhance the rate of Mn^{2+} influx (Figure 8a,b), whereas acetylcholine (100 µM) increased the rate of fluorescence decline (Figure 8b). These data are summarized in Figure 8c and provide the strong evidence that glutamate does not activate metabotropic Ca^{2+} entry in bEND5 cells. It turns out that it is the constitutive SOCE to maintain glutamate-induced intracellular Ca^{2+} oscillations by providing releasable Ca^{2+} to the $InsP_3$-sensitive ER stores (Morgan & Jacob, 1996; Zuccolo, Bottino et al., 2016) and, maybe, to the NAADPsensitive EL Ca^{2+} pool (Sbano et al., 2017).

2.6 | Glutamate-induced intracellular Ca^{2+} oscillations lead to NO release in bEND5 cells

To assess whether glutamate triggers intracellular Ca^{2+} oscillations to drive NO release, bEND5 cells were loaded with the NOsensitive fluorochrome, DAF-FM (Berra-Romani et al., 2013; Mapelli et al., 2017; Zuccolo et al., 2017). Glutamate caused a slow, but sustained increase in NO levels, which started with a latency of 387 ± 53 s (n = 143) and reached a plateau after approximately 1,000 s (Figure 9a). This signal was suppressed by MCPG (200 µM, 10 min; Figure 9a,f). Moreover, glutamate-induced NO release was abolished by preincubating the cells with either L-NG-nitroarginine methyl ester (L-NAME; 100 µM, 1 hr), a widely used eNOS inhibitor, or 1,2-bis(o-aminophenoxy)ethane-N,N,N', N'-tetraacetic acid (BAPTA; 30 µM, 2 hr), a membrane-permeable intracellular Ca^{2+} buffer (Figure 9b,f). Accordingly, BAPTA (30 µM, 2 hr) prevented glutamate-induced intracellular Ca^{2+} oscillations in 75 out of 75 cells (data not shown). These findings demonstrate that glutamate engages eNOS in a Ca^{2+}-dependent manner (Zuccolo, Dragoni et al., 2016; Zuccolo et al., 2017). Unlike acetylcholine (Zuccolo et al., 2017), glutamate-induced NO release also occurred in the absence of external Ca^{2+} and was further enhanced by the subsequent addition of Ca^{2+} to the recording solution (Figure 9c), in agreement with the Ca^{2+} imaging data (Figure 3a). Also, glutamate failed to elevate NO levels in the presence of either U73122 (10 µM, 30 min), and 2-APB (50 µM, 30 min; Figure 9d,f). Finally, glutamate-induced NO release was also inhibited by Ned-19 (10 µM, 30 min; Figure 9e,f) or nigericin (50 µM, 20 min; Figure 9e,f). Collectively, these findings clearly show that glutamate stimulates NO release by activating intracellular Ca^{2+} oscillations in mouse brain endothelial cells.

2.7 | Glutamate induces Ca^{2+}-dependent NO release in human brain microvascular endothelial cells

Finally, we assessed whether glutamate triggers intracellular Ca^{2+} signaling and NO release also in hCMEC/D3, which represents a widely used human brain microvascular endothelial cell line (Re et al., 2011; Zuccolo et al., 2017). We found that glutamate (100 µM) caused an initial increase in $[Ca^{2+}]_i$, which then decayed to resting levels in the continuous presence of the agonist, in 89 out of 89 cells (Figure 10a). Moreover, glutamate (100 µM) caused a robust elevation in DAF-FM fluorescence that was strongly reduced by BAPTA (30 µM, 2 hr; Figure 10b).

Therefore, glutamate triggers Ca^{2+}-dependent NO release also in human microvascular endothelial cells, although by inducing a different Ca^{2+} signature.

3 | DISCUSSION

Herein, we demonstrated for the first time that the excitatory neurotransmitter glutamate triggered metabotropic intracellular Ca^{2+} oscillations and delayed NO release in mouse brain microvascular endothelial cells. This delayed NO signal is likely to play a crucial role in the slower vasodilation that often follows brief neuronal activity or that sustains functional hyperemia during persistent synaptic transmission (Cauli & Hamel, 2010; Hillman, 2014). Moreover, endothelial-dependent NO release could maintain the cerebral vascular tone during the so-called infra-slow oscillations (ISOs) which generate the functional magnetic resonance imaging (fMRI) blood oxygenation level dependent (BOLD) signal in the brain (Hughes, Lorincz, Parri, & Crunelli, 2011; Lorincz, Geall, Bao, Crunelli, & Hughes, 2009). Alternatively, glutamate-induced NO release could play a permissive role in PGE2- or EET-dependent vasodilation (Cauli & Hamel, 2010; LeMaistre et al., 2012). These findings, therefore, shed novel light on the role played by brain microvascular endothelial cells during NVC (Guerra et al., 2018), which represents the cellular and molecular correlate of blood oxygenation level dependent signals in the brain (Hughes et al., 2011; Lorincz et al., 2009).

Glutamate has long been known to induce an NMDAR-mediated increase in $[Ca^{2+}]_i$ in different types of brain microvascular endothelial cells, such as ECV304 (Kuhlmann et al., 2009), primary mouse brain endothelial cells (Legros et al., 2009), and human brain endothelial cells (Sharp et al., 2003). However, this increase in $[Ca^{2+}]_i$ has often been observed at a rather high glutamate concentration, that is approximately equal to 1 mM, as the recording solutions were lacking the glutamate coagonists, glycine or D-serine, which are strictly required by NMDARs to mediate Ca^{2+} entry at physiological glutamate levels also in nonneuronal cells (Hogan-Cann & Anderson, 2016). Accordingly, a recent series of studies demonstrated that, in the presence of D-serine, 10 μM was sufficient to cause NMDAR-mediated, NO-dependent vasodilation in mouse brain microvessels (LeMaistre et al., 2012; Lu et al., 2017). In the present ER: endoplasmic reticulum; PLC: phospholipase Cβ; SE: standard error

investigation, we did not add either glycine or d-serine to the perfusate; moreover, we applied lower micromolar doses of glutamate to prevent NMDAR activation and rule out any contribution from ionotropic glutamate receptors. Under these conditions, glutamate triggered a dose-dependent oscillatory increase in $[Ca^{2+}]_i$ that was due to the activation of metabotropic Ca^{2+}-permeable channels. The following observations strongly support this

conclusion. First, glutamate-induced intracellular Ca^{2+} oscillations were inhibited by the broad-spectrum mGluR antagonist, MCPG. Second, the oscillatory response to glutamate arose in the absence of extracellular Ca^{2+}, which reflects the engagement of metabotropic receptors on the plasma membrane (He, Linden, & Sapirstein, 2012). Third, glutamate-induced intracellular Ca^{2+} waves were mediated by NAADP and $InsP_3$ (see below), which are both synthesized in response to mGluR activation (Attwell et al., 2010; Pandey et al., 2009). Fourth, previous studies reported mGluR expression in several types of brain microvascular endothelial cells (Beard et al., 2012; Collard et al., 2002; Gillard et al., 2003; Lv et al., 2016). The dose-response relationship revealed that 200 µM glutamate was the most efficient dose to evoke intracellular Ca^{2+} oscillations. This result gains a strong functional relevance as glutamate concentration rapidly raise well within this range in the synaptic cleft in response to high frequency stimulation (Clements, Lester, Tong, Jahr, & Westbrook, 1992; Lee et al., 2007). Considering that glutamatergic terminals establish close contacts with parenchymal microvessels (Cauli & Hamel, 2010; Iadecola, 2004), it is highly conceivable that brain microvascular endothelial cells are exposed to a concentration of glutamate which is able to induce robust Ca^{2+} oscillations during neuronal activity.

The following pieces of evidence indicate that glutamate-induced intracellular Ca^{2+} oscillations were supported by rhythmical Ca^{2+} discharge from the $InsP_3$- and NAADP-dependent Ca^{2+} stores and were maintained by constitutive SOCE. First, the oscillatory response was abrogated by inhibiting PLCβ with U73122 and $InsP_3$Rs with 2-APB (Dragoni, Reforgiato et al., 2015; Potenza et al., 2014). 2-APB is not a specific $InsP_3$R blocker (Moccia, Dragoni et al., 2014; Moccia et al., 2016), but these experiments were carried out under $0Ca^{2+}$ conditions to prevent any contaminating effect from the blockade of Ca^{2+} entry pathways (Dragoni et al., 2011). Of note, a recent analysis of the Ca^{2+} toolkit expressed by bEND5 cells revealed that they are endowed with $InsP_3$R1 and $InsP_3$R2 (Zuccolo et al., 2017), which are the most $InsP_3$ sensitive isoforms and whose assortment represents the most suitable combination to generate periodic cycles of ER Ca^{2+} release (Mikoshiba, 2007; Miyakawa et al., 1999). Second, depleting the ER CA^{2+} pool with the selective SERCA inhibitor, CPA, prevented the subsequent Ca^{2+} response to glutamate (Potenza et al., 2014). Likewise, the application of CPA to ongoing glutamate-induced intracellular Ca^{2+} waves resulted in the complete suppression of Ca^{2+} activity. As discussed in (Zuccolo et al., 2017), this observation indicates that ER-released Ca^{2+} must be sequestered back into ER lumen to set up the next cycle of Ca^{2+} release. Third, RyRs, which may amplify $InsP_3$-dependent Ca^{2+} release through the Ca^{2+}-induced Ca^{2+} release (CICR) mechanism in vascular endothelial cells (Moccia, Tanzi, & Munaron, 2014), are absent in bEND5 cells (Zuccolo et al., 2017). Fourth, the onset of glutamate-induced intracellular Ca^{2+} oscillations was inhibited by NED-19, a rather selective inhibitor of NAADP-induced intracellular Ca^{2+} mobilization (Di Nezza et al., 2017; Pitt et al., 2016), and by depleting the EL Ca^{2+} store with nigericin (Morgan et al., 2011; Patel & Docampo, 2010). Moreover, bEND5 cells express both NAADP-gated channels, TPC1 and TPC2. Consistent with these observations, exogenously delivered NAADP triggered robust intracellular Ca^{2+} mobilization, that was inhibited by either NED-19 or nigericin. NAADP gates TPCs to evoke a local "trigger" Ca^{2+} release from the EL Ca^{2+} store which is in turn

amplified by adjoining ER-embedded InsP$_3$Rs and/or RyRs through the CICR process (Galione, 2015; Moccia, Nusco, Lim, Kyozuka, & Santella, 2006; Morgan, 2016; Ronco et al., 2015). Of note, glutamate has recently been shown to recruit the acidic Ca^{2+} stores by activating TPC1 and TPC2 in cultured rat hippocampal neurons and astrocytes (Pandey et al., 2009; Pereira et al., 2017). Although this hypothesis remains to be experimentally probed, we propose that NAADP-mediated EL Ca^{2+} release triggers glutamate-induced intracellular Ca^{2+} oscillations also in bEND5 cells. In agreement with this suggestion, earlier work from Galione's group demonstrated that the interaction between NAADP and InsP$_3$/cyclic ADP ribose (cADPr) is the most suitable mechanism to generate repetitive oscillations in [Ca^{2+}]$_i$ via the two-pool (i.e. EL and ER Ca^{2+} stores) mechanism (Cancela, 2001; Cancela, Churchill, & Galione, 1999; Churchill & Galione, 2001).

Glutamate-induced intracellular Ca^{2+} oscillations were maintained over time by extracellular Ca^{2+} entry. Accordingly, ongoing Ca^{2+} transients were rapidly abolished in the absence of Ca^{2+} entry with only 1–2 spikes occurring after extracellular Ca^{2+} removal. This feature is consistent with the notion that endogenous Ca^{2+} release is required to support the cycling Ca^{2+} activity and that extracellular Ca^{2+} is required to maintain the oscillations throughout glutamate stimulation. Quite surprisingly, the Mn^{2+}-quenching technique revealed that glutamate failed to cause any resolvable decrease in the rate of divalent cation entry. This result strongly suggests that the metabotropic signal delivered by glutamate was not able to recruit plasmalemmal Ca^{2+}-permeable channels, although we cannot rule out the possibility that glutamate gates a Mn^{2+}-impermeable nonselective cation channel. Therefore, we hypothesize that, unlike acetylcholine (Zuccolo et al., 2017), the InsP$_3$-sensitive ER Ca^{2+} pool targeted by glutamate is not coupled to store-operated Ca^{2+} channels, yet it requires constitutive SOCE to be refilled during prolonged stimulation. In agreement with this mode, our previous study clearly showed that constitutive SOCE replenished the ER with Ca^{2+} under resting conditions (Zuccolo et al., 2017). Because glutamate did not elicit detectable Ca^{2+} entry, but extracellular Ca^{2+} entry was indispensable for maintaining the oscillations over time, constitutive Ca^{2+} entry is the most likely candidate to restore the glutamate-sensitive ER Ca^{2+} pool. Earlier investigations demonstrated

that the degree of SOCE activation may be agonist-dependent in microvascular endothelial cells (Moccia, Berra-Romani, & Tanzi, 2012). For instance, epidermal growth factor, but not ATP, was able to activate SOCE in rat cardiac microvascular endothelial cells (Moccia et al., 2001; Moccia et al., 2003). Likewise, protease-activated receptor-1 induced SOCE in mouse microvascular endothelial cells (Sundivakkam, Natarajan, Malik, & Tiruppathi, 2013), whereas massive depletion of the ER Ca^{2+} pool with thapsigargin did not elicit Ca^{2+} influx in the same cells (Kelly et al., 1998). These observations concur with the notion that the ER microenvironment is not homogeneous and that the ER presents distinct autonomous modular units that fulfill different tasks (Berridge, 2002). Accordingly, it has long been known that ER-dependent Ca^{2+} release may occur without activating concomitant Ca^{2+} entry (Parekh & Putney, 2005). This peculiar feature depends on the existence of distinct InsP$_3$sensitive ER subcompartments, some of which are coupled to SOCE, whereas others are not (Parekh & Putney, 2005). Intriguingly, glutamate was previously found to inhibit constitutive Ca^{2+} entry (and NO release) in rat bone marrow

stromal cells (Foreman, Gu, Howl, Jones, & Publicover, 2005), but this mechanism seems to be inactive in bEND5 cells.

Oscillations in $[Ca^{2+}]_i$ have long been known to stimulate eNOS to produce NO in endothelial cells from several vascular beds (Kasai, Yamazawa, Sakurai, Taketani, & Iino, 1997; Sandow, Senadheera, Grayson, Welsh, & Murphy, 2012), including bEND5 cells (Zuccolo et al., 2017). The extent of NO release may be finely tuned by adjusting the frequency of Ca^{2+} spikes (Zuccolo et al., 2017), which provides a reliable mechanism to regulate the activity of a cellular decoder, such as eNOS, that integrates repetitive Ca^{2+} signals in a highly cooperative manner (Smedler & Uhlen, 2014). Glutamateevoked NO release was abrogated by inhibiting Group I mGluRs with MCPG and by blocking each component of the Ca^{2+} toolkit involved in the generation of the Ca^{2+} spikes, that is the $InsP_3$- and NAADPdependent signaling pathways. Unlike acetylcholine (Zuccolo et al., 2017), however, the increase in NO levels was detectable at around 300 s after the onset of glutamate-induced Ca^{2+} waves and reached its peak with rather slow kinetics. Therefore, although both agonists induce intracellular Ca^{2+} oscillations, eNOS sensitivity to the Ca^{2+}-dependent stimulation differs between acetylcholine and glutamate. This difference has already been reported in endothelial cells covering pig aortic valves, in which, for a given increase in $[Ca^{2+}]_i$, the extent NO production varied depending on the extracellular agonist (thrombin > ATP > bradykinin > ionomycin; Mizuno et al., 2000). The highest frequency of glutamate-induced intracellular Ca^{2+} oscillations falls within the same range as that described for acetylcholine (≈0.0045 Hz vs. ≈0.0047 Hz). Therefore, as suggested for endothelial cells ex vivo (Mizuno et al., 2000), we speculate that Ca^{2+} transients interact with other signaling pathways to affect eNOS activation in glutamate-stimulated cells (Mancardi, Pla, Moccia, Tanzi, & Munaron, 2011). For instance, Akt/protein kinase B (PKB) promotes NO release independently on Ca^{2+} by phosphorylating eNOS (Siragusa & Fleming, 2016). Interestingly, Group 1 mGluRs may enhance angiogenesis by recruiting the phosphoinositide 3-kinase (PI3K)/PKB pathway (Wen et al., 2014). It should, however, be recalled that DAF-FM is not a true NO detector, but is rather sensitive to several nitrogen derivatives, such as N2O3, NO2, or ONOO (Hall & Garthwaite, 2009). More specifically, NO seems to react with the NH radical of the fluorophore which is generated by its nonspecific oxidation (Hall & Garthwaite, 2009). Therefore, NO levels could start to increase before they become detectable through an increase in

This finding indicates that a basal Ca^{2+}-permeable pathway is active in the former, but not in the latter. The rate of fluorescence decay for each individual tracing was calculated as the slope of linear regression. Glutamate (Glu) addition did not enhance the rate of Mn^{2+} entry, thereby suggesting that Glu does not activate any Ca^{2+}- and Mn^{2+}-permeable pathway under these conditions in bEND5 cells. (b) Ach (300 μM) caused a clear increase in the rate of Mn^{2+} entry in bEND5 cells, whereas Glu was ineffective. (c) Average ± SE of the quenching rate of Fura-2 fluorescence signal measured in bEND5 cells under resting conditions and on Glu stimulation. The asterisk indicates $p < 0.05$. PSS: physiological salt solution; SOCE: store-operated Ca2+ entry; SE: standard error DAF-FM fluorescence. An additional caveat that should be taken in consideration is that replacing the extracellular perfusate with a glutamate-containing solution does not faithfully mimic the physiological conditions during which glutamate is delivered onto brain microvascular endothelial cells, that is synaptic activity. Glutamatergic terminals are in close proximity and functionally coupled to adjoining parenchymal microvessels (Cauli & Hamel, 2010; Iadecola, 2004). Therefore, brain microvascular endothelial cells are in the most suitable location to directly sense neuronal activity provided that they are endowed with mGluRs (or NMDARs). The frequency of the Ca^{2+} spikes we observed was even lower of the slower (0.5–1 Hz) brain oscillations that occur during deep sleep (Berridge, 2014). However, we envisage that high frequency (80–100 Hz) synaptic transmission in vivo could accelerate the frequency of the endothelial Ca^{2+} waves, thereby anticipating the onset of the ensuing NO signal. Nevertheless, glutamate-induced endothelial NO release is unlikely to mediate the fast NO-dependent vasodilation that follows neuronal activity in cerebellum and hippocampus (Cauli & Hamel, 2010; Mapelli et al., 2017). Conversely, the delayed endothelial NO signal could underpin the slower component of the vasodilating response to brief neuronal activity in these structures (Hillman, 2014; Lourenco et al., 2017; Mapelli et al., 2017) or play a permissive role in the PGE2- or EET-dependent vasodilation that occurs during sustained (up to 1 min) synaptic activation in the cortex (Cauli & Hamel, 2010; LeMaistre et al., 2012). Future in vivo experiments, involving the use of transgenic mice expressing genetic Ca^{2+} biosensors (such as GCaMP2) in vascular endothelium (Sonkusare et al., 2012) and of more sensitive tools for NO detection (such as electrochemical probes; Maffei et al., 2003), will be necessary to address the exact role of glutamate-induced eNOS activation in NVC. In must, however, be pointed out that very slow or ISOs well below 0.1 Hz (0.005–0.1 Hz) occur in the thalamus, as well as in other cortical structures, and are driven by mGluR activation (Hughes et al., 2011; Lorincz et al., 2009). Of note, these ISOs have been associated to the spontaneous <0.1 Hz bloodoxygen-dependent level (BOLD) signals recorded with fMRI in resting individuals (Hughes et al., 2011). The cellular and biochemical underpinnings of such low-frequency BOLD fluctuations, which provide one of the most efficient tools to map brain connectivity, are yet to be elucidated. Intriguingly, the novel observation that lowfrequency glutamate-induced intracellular Ca^{2+} waves in brain microvascular endothelial cells lead to robust NO release could shed new light on the underlying mechanism. Nevertheless, our preliminary data indicated that glutamate-induced Ca^{2+}-dependent NO release is quite faster in hCMEC/D3 cells, an established cell line of human brain microvascular endothelial cells. This finding remains to be confirmed, but endorses the view that subtle differences in the Ca^{2+} signaling machinery lead to different functional outcomes in endothelial cells from different species (Moccia et al., 2012; Zuccolo et al., 2018). Finally, we have to recall that intracellular Ca^{2+}

drives the synthesis of a plethora of endothelial-derived vasorelaxing messengers, including PGE2, EETs, and hydrogen sulfide, and triggers endothelium-dependent hyperpolarization (EDH; Altaany, Moccia, Munaron, Mancardi, & Wang, 2014; Attwell et al., 2010; Guerra et al., 2018). Therefore, future experiments will be necessary to assess whether the signaling pathway we described in the present investigation contributes to generate PGE2 and/or EETs in the brain areas, such as the cortex, in which these vasoactive factors trigger the vasodilating response to glutamatergic transmission (Cauli & Hamel, 2010; Lecrux & Hamel, 2016). Likewise, glutamateinduced intracellular Ca^{2+} waves could recruit intermediate- and small-conductance Ca^{2+}-dependent K^+ channels (SK_{Ca} and IK_{Ca}, respectively), which mediate EDH (Behringer, 2017). Finally, glutamate could be massively released on traumatic brain injury, thereby promoting aberrant neuronal signaling and contributing to neurological deficits (Hinzman et al., 2010). Intracellular Ca^{2+} oscillations may promote the re-endothelialization process of injured vessels (Berra-Romani et al., 2012; Zhao, Walczysko, & Zhao, 2008). Glutamate-induced intracellular Ca^{2+} oscillations could sustain proliferation and migration in brain microvascular endothelial cells which are located in the proximity of the damaged area.

In conclusion, glutamate induces intracellular Ca^{2+} oscillations in mouse brain endothelial cells, thereby triggering robust, although delayed, NO release. This finding further corroborates the notion that brain microvascular endothelial cells may directly sense synaptically

released neurotransmitters, for example, acetylcholine and glutamate, and play an active role in NVC (B. R. Chen et al., 2014; Hillman, 2014; LeMaistre et al., 2012; Stobart et al., 2013; Zuccolo et al., 2017). Recent evidence suggested that several neurodegenerative disorders, including Alzheimer's disease (AD), are triggered by vascular, rather than neuronal, dysfunction (Iadecola, 2004; Iadecola, 2017). Interestingly, the intracellular Ca^{2+} toolkit is severely compromised in rat brain microvascular endothelial cells exposed to amyloid-beta (Aβ) peptide (Fonseca et al., 2015), whose accumulation in brain parenchyma and in the cerebrovasculature represents a major pathogenic factor in AD (Iadecola, 2017). Future studies will have to assess whether and how Aβ peptide affects glutamate-induced Ca^{2+} signaling and NO release in brain microvascular endothelium.

ORCID

Elia Ranzato   http://orcid.org/0000-0002-7600-8215 Francesco Moccia   http://orcid.org/0000-0003-0010-0098

REFERENCES

Altaany, Z., Moccia, F., Munaron, L., Mancardi, D., & Wang, R. (2014). Hydrogen sulfide and endothelial dysfunction: Relationship with nitric oxide. Current Medicinal Chemistry, 21(32), 3646–3661.

Andresen, J., Shafi, N. I., & Bryan, R. M., Jr. (2006). Endothelial influences on cerebrovascular tone. Journal of Applied Physiology (1985), 100(1), 318–327.

Attwell, D., Buchan, A. M., Charpak, S., Lauritzen, M., Macvicar, B. A., & Newman, E. A. (2010). Glial and neuronal control of brain blood flow.
Nature, 468(7321), 232–243.

Beard, R. S., Jr., Reynolds, J. J., & Bearden, S. E. (2012). Metabotropic glutamate receptor 5 mediates phosphorylation of vascular endothelial cadherin and nuclear localization of beta-catenin in response to homocysteine. Vascular Pharmacology, 56(3-4), 159–167.

Behringer, E. J. (2017). Calcium and electrical signaling in arterial endothelial tubes: New insights into cellular physiology and cardiovascular function. Microcirculation, 24(3), e12328.

Berra-Romani, R., Avelino-Cruz, J. E., Raqeeb, A., Della Corte, A., Cinelli, M., Montagnani, S., … Tanzi, F. (2013). Ca(2)(+)-dependent nitric oxide release in the injured endothelium of excised rat aorta: A promising mechanism applying in vascular prosthetic devices in aging patients.
BMC Surgery, 13(Suppl 2), S40.

Berra-Romani, R., Raqeeb, A., Torres-Jácome, J., Guzman-Silva, A., Guerra, G., Tanzi, F., & Moccia, F. (2012). The mechanism of injuryinduced intracellular calcium concentration oscillations in the endothelium of excised rat aorta. Journal of Vascular Research, 49 (1), 65–76.

Berridge, M. J. (2002). The endoplasmic reticulum: A multifunctional signaling organelle. Cell Calcium, 32(5-6), 235–249.

Berridge, M. J. (2014). Calcium regulation of neural rhythms, memory and Alzheimer's disease. Journal of Physiology, 592(2), 281–293.

Bird, G. S. J., & Putney, J. W., Jr. (2005). Capacitative calcium entry supports calcium oscillations in human embryonic kidney cells. Journal of Physiology, 562(Pt 3), 697–706.

Brailoiu, G. C., Gurzu, B., Gao, X., Parkesh, R., Aley, P. K., Trifa, D. I., … Brailoiu, E. (2010). Acidic NAADP-sensitive calcium stores in the endothelium: Agonist-specific recruitment and role in regulating blood pressure. Journal of Biological Chemistry, 285(48), 37133–37137. Bufalo, G., Di Nezza, F., Cimmino, L., Cuomo, F., & Ambrosone, L. (2017). Physicochemical investigation of ultrasound effects on some steps of mink fur processing. A suggestion for improving the worker health and reducing the environmental impact. Journal of Cleaner Production, 143, 10–16.

Calcinaghi, N., Jolivet, R., Wyss, M. T., Ametamey, S. M., Gasparini, F., Buck, A., & Weber, B. (2011). Metabotropic glutamate receptor mGluR5 is not involved in the early hemodynamic response. Journal of Cerebral Blood Flow and Metabolism, 31(9), e1–e10.

Cancela, J. M. (2001). Specific Ca2+ signaling evoked by cholecystokinin and acetylcholine: The roles of NAADP, cADPR, and IP3. Annual Review of Physiology, 63, 99–117.

Cancela, J. M., Churchill, G. C., & Galione, A. (1999). Coordination of agonist-induced Ca2+-signalling patterns by NAADP in pancreatic acinar cells. Nature, 398(6722), 74–76.

Cauli, B., & Hamel, E. (2010). Revisiting the role of neurons in neurovascular coupling. Frontiers in Neuroenergetics, 2, 9.

Chen, B. R., Kozberg, M. G., Bouchard, M. B., Shaik, M. A., & Hillman, E. M. C. (2014). A critical role for the vascular endothelium in functional neurovascular coupling in the brain. Journal of the American Heart Association, 3(3), e000787.

Chen, J. B., Tao, R., Sun, H. Y., Tse, H. F., Lau, C. P., & Li, G. R. (2010). Multiple Ca2+ signaling pathways regulate intracellular Ca2+ activity in human cardiac fibroblasts. Journal of Cellular Physiology, 223(1), 68–75.

Churchill, G. C., & Galione, A. (2001). NAADP induces Ca2+ oscillations via a two-pool mechanism by priming IP3- and cADPR-sensitive Ca2+ stores. EMBO Journal, 20(11), 2666–2671.

Clements, J., Lester, R., Tong, G., Jahr, C., & Westbrook, G. (1992). The time course of glutamate in the synaptic cleft. Science, 258(5087), 1498–1501.

Collard, C. D., Park, K. A., Montalto, M. C., Alapati, S., Buras, J. A., Stahl, G. L., & Colgan, S. P. (2002). Neutrophil-derived glutamate regulates vascular endothelial barrier function. Journal of Biological Chemistry, 277(17), 14801–14811.

Dai, J. M., Kuo, K. H., Leo, J. M., van Breemen, C., & Lee, C. H. (2006). Mechanism of ACh-induced asynchronous calcium waves and tonic contraction in porcine tracheal muscle bundle. American Journal of Physiology: Lung Cellular and Molecular Physiology, 290(3), L459–L469.

De Bock, M., Culot, M., Wang, N., Bol, M., Decrock, E., De Vuyst, E., … Leybaert, L. (2011). Connexin channels provide a target to manipulate brain endothelial calcium dynamics and blood-brain barrier permeability. Journal of Cerebral Blood Flow and Metabolism, 31(9), 1942–1957.

De Bock, M., Wang, N., Decrock, E., Bol, M., Gadicherla, A. K., Culot, M., … Leybaert, L. (2013). Endothelial calcium dynamics, connexin channels and blood-brain barrier function. Progress in Neurobiology, 108, 1–20.

Di, A., & Malik, A. B. (2010). TRP channels and the control of vascular function. Current Opinion in Pharmacology, 10(2), 127–132.

Dragoni, S., Guerra, G., Pla, A. F., Bertoni, G., Rappa, A., Poletto, V., … Moccia, F. (2015). A functional transient receptor potential vanilloid 4 (TRPV4) channel is expressed in human endothelial progenitor cells. Journal of Cellular Physiology, 230(1), 95–104.

Dragoni, S., Laforenza, U., Bonetti, E., Lodola, F., Bottino, C., Berra-Romani, R., … Moccia, F. (2011). Vascular endothelial growth factor stimulates endothelial colony forming cells proliferation and tubulogenesis by inducing oscillations in intracellular Ca2+ concentration. Stem Cells, 29(11), 1898–1907.

Dragoni, S., Reforgiato, M., Zuccolo, E., Poletto, V., Lodola, F., Ruffinatti, F. A., … Moccia, F. (2015). Dysregulation of VEGF-induced proangiogenic Ca2+ oscillations in primary myelofibrosis-derived endothelial colonyforming cells. Experimental Hematology, 43(12), 1019–1030. e1013.

Duncker, D. J., & Bache, R. J. (2008). Regulation of coronary blood flow during exercise. Physiological Reviews, 88(3), 1009–1086.

Favia, A., Desideri, M., Gambara, G., D'Alessio, A., Ruas, M., Esposito, B., … Filippini, A. (2014). VEGF-induced neoangiogenesis is mediated by NAADP and two-pore channel-2-dependent Ca2+ signaling. Proceedings of the National Academy of Sciences of the United States of America, 111(44), E4706–E4715.

Feng, M., Grice, D. M., Faddy, H. M., Nguyen, N., Leitch, S., Wang, Y., … Rao, R. (2010). Store-independent activation of Orai1 by SPCA2 in mammary tumors. Cell, 143(1), 84–98.

Fonseca, A. C. R. G., Moreira, P. I., Oliveira, C. R., Cardoso, S. M., Pinton, P., & Pereira, C. F. (2015). Amyloid-beta disrupts calcium and redox homeostasis in brain endothelial cells. Molecular Neurobiology, 51(2), 610–622.

Foreman, M. A., Gu, Y., Howl, J. D., Jones, S., & Publicover, S. J. (2005). Group III metabotropic glutamate receptor activation inhibits Ca2+ influx and nitric oxide synthase activity in bone marrow stromal cells. Journal of Cellular Physiology, 204(2), 704–713.

Galione, A. (2015). A primer of NAADP-mediated Ca(2+) signalling: From sea urchin eggs to mammalian cells. Cell Calcium, 58(1), 27–47.

Gambara, G., Billington, R. A., Debidda, M., D'Alessio, A., Palombi, F., Ziparo, E., … Filippini, A. (2008). NAADP-induced Ca(2+ signaling in response to endothelin is via the receptor subtype B and requires the integrity of lipid rafts/caveolae. Journal of Cellular Physiology, 216(2), 396–404.

Gillard, S. E., Tzaferis, J., Tsui, H. C. T., & Kingston, A. E. (2003). Expression of metabotropic glutamate receptors in rat meningeal and brain microvasculature and choroid plexus. Journal of Comparative Neurology, 461(3), 317–332.

Guerra, G., Lucariello, A., Perna, A., Botta, L., De Luca, A., & Moccia, F. (2018). The role of endothelial Ca(2+) signaling in neurovascular coupling: A view from the lumen. International Journal of Molecular Sciences, 19(4), 938.

Guse, A. H. (2012). Linking NAADP to ion channel activity: A unifying hypothesis. Science Signaling, 5(221), pe18.

Hall, C. N., & Garthwaite, J. (2009). What is the real physiological NO concentration in vivo? Nitric oxide, 21(2), 92–103.

Hall, C. N., Reynell, C., Gesslein, B., Hamilton, N. B., Mishra, A., Sutherland, B. A., … Attwell, D. (2014). Capillary pericytes regulate cerebral blood flow in health and disease. Nature, 508(7494), 55–60.

Hallam, T. J., Jacob, R., & Merritt, J. E. (1988). Evidence that agonists stimulate bivalent-cation influx into human endothelial cells. Biochemical Journal, 255(1), 179–184.

Hamel, E. (2006). Perivascular nerves and the regulation of cerebrovascular tone. Journal of Applied Physiology, 100(3), 1059–1064.

He, L., Linden, D. J., & Sapirstein, A. (2012). Astrocyte inositol triphosphate receptor type 2 and cytosolic phospholipase A2 alpha regulate arteriole responses in mouse neocortical brain slices. PLoS One, 7(8), e42194.

Hillman, E. M. C. (2014). Coupling mechanism and significance of the BOLD signal: A status report. Annual Review of Neuroscience, 37, 161–181.

Hinzman, J. M., Thomas, T. C., Burmeister, J. J., Quintero, J. E., Huettl, P., Pomerleau, F., … Lifshitz, J. (2010). Diffuse brain injury elevates tonic glutamate levels and potassium-evoked glutamate release in discrete brain regions at two days post-injury: An enzyme-based microelectrode array study. Journal of Neurotrauma, 27(5), 889–899.

Hogan-Cann, A. D., & Anderson, C. M. (2016). Physiological roles of nonneuronal NMDA receptors. Trends In Pharmacological Sciences, 37(9), 750–767.

Hughes, S. W., Lorincz, M. L., Parri, H. R., & Crunelli, V. (2011). Infraslow (<0.1 Hz) oscillations in thalamic relay nuclei basic mechanisms and significance to health and disease states. Progress in Brain Research, 193, 145–162.

Iadecola, C. (2004). Neurovascular regulation in the normal brain and in Alzheimer's disease. Nature Reviews Neuroscience, 5(5), 347–360.

Iadecola, C. (2017). The neurovascular unit coming of age: A journey through neurovascular coupling in health and disease. Neuron, 96(1), 17–42.

Jacob, R. (1990). Agonist-stimulated divalent cation entry into single cultured human umbilical vein endothelial cells. Journal of Physiology, 421, 55–77.

Kasai, Y., Yamazawa, T., Sakurai, T., Taketani, Y., & Iino, M. (1997). Endothelium-dependent frequency modulation of Ca2+ signalling in individual vascular smooth muscle cells of the rat. Journal of Physiology, 504(Pt 2), 349–357.

Kelly, J. J., Moore, T. M., Babal, P., Diwan, A. H., Stevens, T., & Thompson,

W. J. (1998). Pulmonary microvascular and macrovascular endothelial cells: Differential regulation of Ca2+ and permeability. American Journal of Physiology, 274(5 Pt 1), L810–L819.

Kisler, K., Nelson, A. R., Montagne, A., & Zlokovic, B. V. (2017). Cerebral blood flow regulation and neurovascular dysfunction in Alzheimer disease. Nature Reviews Neuroscience, 18(7), 419–434.

Kuhlmann, C. R. W., Zehendner, C. M., Gerigk, M., Closhen, D., Bender, B., Friedl, P., & Luhmann, H. J. (2009). MK801 blocks hypoxic bloodbrain-barrier disruption and leukocyte adhesion. Neuroscience Letters, 449(3), 168–172.

Lauritzen, M., Mathiesen, C., Schaefer, K., & Thomsen, K. J. (2012). Neuronal inhibition and excitation, and the dichotomic control of brain hemodynamic and oxygen responses. NeuroImage, 62(2), 1040–1050.

Lecrux, C., & Hamel, E. (2016). Neuronal networks and mediators of cortical neurovascular coupling responses in normal and altered brain states. Philosophical Transactions of the Royal Society of London. Series B, Biological Sciences, 371(1705), 20150350.

Lecrux, C., Toussay, X., Kocharyan, A., Fernandes, P., Neupane, S., Levesque, M., … Hamel, E. (2011). Pyramidal neurons are "neurogenic hubs" in the neurovascular coupling response to whisker stimulation. Journal of Neuroscience, 31(27), 9836–9847.

Lee, K. H., Kristic, K., van Hoff, R., Hitti, F. L., Blaha, C., Harris, B., … Leiter, J. C. (2007). High-frequency stimulation of the subthalamic nucleus increases glutamate in the subthalamic nucleus of rats as demonstrated by in vivo enzyme-linked glutamate sensor. Brain Research, 1162, 121–129.

Legros, H., Launay, S., Roussel, B. D., Marcou-Labarre, A., Calbo, S., Catteau, J., … Laudenbach, V. (2009). Newborn- and adult-derived brain microvascular endothelial cells show age-related differences in phenotype and glutamate-evoked protease release. Journal of Cerebral Blood Flow and Metabolism, 29(6), 1146–1158.

LeMaistre, J. L., Sanders, S. A., Stobart, M. J., Lu, L., Knox, J. D., Anderson, H. D., & Anderson, C. M. (2012). Coactivation of NMDA receptors by glutamate and $_D$-serine induces dilation of isolated middle cerebral arteries. Journal of Cerebral Blood Flow and Metabolism, 32(3), 537–547.

Lim, D., Iyer, A., Ronco, V., Grolla, A. A., Canonico, P. L., Aronica, E., & Genazzani, A. A. (2013). Amyloid beta deregulates astroglial mGluR5mediated calcium signaling via calcineurin and Nf-kB. GLIA, 61(7), 1134–1145.

Lourenço, C. F., Ledo, A., Barbosa, R. M., & Laranjinha, J. (2017). Neurovascular-neuroenergetic coupling axis in the brain: Master regulation by nitric oxide and consequences in aging and neurodegeneration. Free Radical Biology and Medicine, 108, 668–682.

Lu, L., Hogan-Cann, A. D., Globa, A. K., Lu, P., Nagy, J. I., Bamji, S. X., & Anderson, C. M. (2017). Astrocytes drive cortical vasodilatory signaling by activating endothelial NMDA receptors. Journal of Cerebral Blood Flow and Metabolism, 271678X17734100.

Lv, J. M., Guo, X. M., Chen, B., Lei, Q., Pan, Y. J., & Yang, Q. (2016). The noncompetitive AMPAR antagonist perampanel abrogates brain endothelial cell permeability in response to ischemia: Involvement of claudin-5. Cellular and Molecular Neurobiology, 36(5), 745–753.

Lörincz, M. L., Geall, F., Bao, Y., Crunelli, V., & Hughes, S. W. (2009). ATPdependent infra-slow (<0.1 Hz) oscillations in thalamic networks. PLoS One, 4(2), e4447.

Maffei, A., Prestori, F., Shibuki, K., Rossi, P., Taglietti, V., & D'Angelo, E. (2003). NO enhances presynaptic currents during cerebellar mossy fiber-granule cell LTP. Journal of Neurophysiology, 90(4), 2478–2483.

Mancardi, D., Florio pla, A., Moccia, F., Tanzi, F., & Munaron, L. (2011). Old and new gasotransmitters in the cardiovascular system: Focus on the role of nitric oxide and hydrogen sulfide in endothelial cells and cardiomyocytes. Current Pharmaceutical Biotechnology, 12(9), 1406–1415. Mapelli, L., Gagliano, G., Soda, T., Laforenza, U., Moccia, F., & D'Angelo, E. U. (2017). Granular layer neurons control cerebellar neurovascular coupling through an NMDA receptor/NO-dependent system. Journal of Neuroscience, 37(5), 1340–1351.

Melchionda, M., Pittman, J. K., Mayor, R., & Patel, S. (2016). Ca2+/H+ exchange by acidic organelles regulates cell migration in vivo. Journal of Cell Biology, 212(7), 803–813.

Mikoshiba, K. (2007). IP3 receptor/Ca2+ channel: From discovery to new signaling concepts. Journal of Neurochemistry, 102(5), 1426–1446.

Mishra, A. (2017). Binaural blood flow control by astrocytes: Listening to synapses and the vasculature. Journal of Physiology, 595(6), 1885–1902.

Miyakawa, T., Maeda, A., Yamazawa, T., Hirose, K., Kurosaki, T., & Iino, M. (1999). Encoding of Ca2+ signals by differential expression of IP3 receptor subtypes. EMBO Journal, 18(5), 1303–1308.

Mizuno, O., Kobayashi, S., Hirano, K., Nishimura, J., Kubo, C., & Kanaide, H. (2000). Stimulus-specific alteration of the relationship between cytosolic Ca(2+) transients and nitric oxide production in endothelial cells ex vivo. British Journal of Pharmacology, 130(5), 1140–1146.

Moccia, F., Baruffi, S., Spaggiari, S., Coltrini, D., Berra-Romani, R., Signorelli, S., … Tanzi, F. (2001). P2y1 and P2y2 receptor-operated Ca2+ signals in primary cultures of cardiac microvascular endothelial cells. Microvascular Research, 61(3), 240–252.

Moccia, F., Berra-Romani, R., Baruffi, S., Spaggiari, S., Adams, D. J., Taglietti, V., & Tanzi, F. (2002). Basal nonselective cation permeability in rat cardiac microvascular endothelial cells. Microvascular Research, 64(2), 187–197.

Moccia, F., Berra-Romani, R., & Tanzi, F. (2012). Update on vascular endothelial Ca2+ signalling: A tale of ion channels, pumps and transporters. World Journal of Biological Chemistry, 3(7), 127–158.

Moccia, F., Berra-Romani, R., Tritto, S., Signorelli, S., Taglietti, V., & Tanzi, F. (2003). Epidermal growth factor induces intracellular Ca2+ oscillations in microvascular endothelial cells. Journal of Cellular Physiology, 194, 139–150.

Moccia, F., Dragoni, S., Poletto, V., Rosti, V., Tanzi, F., Ganini, C., & Porta, C. (2014). Orai1 and transient receptor potential channels as novel molecular targets to impair tumor neovascularisation in renal cell carcinoma and other malignancies. Anti-Cancer Agents in Medicinal Chemistry, 14(2), 296–312.

Moccia, F., & Guerra, G. (2016). Ca(2+) signalling in endothelial progENITOR Cells: Friend or foe? Journal of Cellular Physiology, 231(2), 314–327.

Moccia, F., Lucariello, A., & Guerra, G. (2018). TRPC3-mediated Ca(2+) signals as a promising strategy to boost therapeutic angiogenesis in failing hearts: The role of autologous endothelial colony forming cells. Journal of Cellular Physiology, 233(5), 3901–3917.

Moccia, F., Nusco, G. A., Lim, D., Kyozuka, K., & Santella, L. (2006). NAADP and InsP3 play distinct roles at fertilization in starfish oocytes. Developmental Biology, 294(1), 24–38.

Moccia, F., Tanzi, F., & Munaron, L. (2014). Endothelial remodelling and intracellular calcium machinery. Current Molecular Medicine, 14(4), 457–480.

Moccia, F., Zuccolo, E., Poletto, V., Turin, I., Guerra, G., Pedrazzoli, P., … Montagna, D. (2016). Targeting stim and orai proteins as an alternative approach in anticancer therapy. Current Medicinal Chemistry, 23(30), 3450–3480.

Morgan, A. J. (2016). Ca2+ dialogue between acidic vesicles and ER.
Biochemical Society Transactions, 44(2), 546–553.

Morgan, A. J., & Jacob, R. (1996). Ca2+ influx does more than provide releasable Ca2+ to maintain repetitive spiking in human umbilical vein endothelial cells. Biochemical Journal, 320(Pt 2), 505–517.

Morgan, A. J., Platt, F. M., Lloyd-Evans, E., & Galione, A. (2011). Molecular mechanisms of endolysosomal Ca2+ signalling in health and disease.
Biochemical Journal, 439(3), 349–374.

Di Nezza, F., Zuccolo, E., Poletto, V., Rosti, V., De Luca, A., Moccia, F., … Ambrosone, L. (2017). liposomes as a putative tool to investigate NAADP signaling in vasculogenesis. Journal of Cellular Biochemistry, 118, 3722–3729.

Pandey, V., Chuang, C. C., Lewis, A. M., Aley, P. K., Brailoiu, E., Dun, N. J., … Patel, S. (2009). Recruitment of NAADP-sensitive acidic Ca2+ stores by glutamate. Biochemical Journal, 422(3), 503–512.

Parekh, A. B., & Putney, J. W., Jr. (2005). Store-operated calcium channels.
Physiological Reviews, 85(2), 757–810.

Patel, S. (2015). Function and dysfunction of two-pore channels. Science Signaling, 8(384), re7.

Patel, S., & Docampo, R. (2010). Acidic calcium stores open for business: Expanding the potential for intracellular Ca2+ signaling. Trends in Cell Biology, 20(5), 277–286.

Pereira, G. J. S., Antonioli, M., Hirata, H., Ureshino, R. P., Nascimento, A. R., Bincoletto, C., … Smaili, S. S. (2017). Glutamate induces autophagy via the two-pore channels in neural cells. Oncotarget, 8(8), 12730–12740. Pitt, S. J., Reilly-O'Donnell, B., & Sitsapesan, R. (2016). Exploring the biophysical evidence that mammalian two-pore channels are NAADPactivated calcium-permeable channels. Journal of Physiology, 594(15), 4171–4179.

Potenza, D. M., Guerra, G., Avanzato, D., Poletto, V., Pareek, S., Guido, D., … Moccia, F. (2014). Hydrogen sulphide triggers VEGF-induced intracellular Ca(2+) signals in human endothelial cells but not in their immature progenitors. Cell Calcium, 56, 225–234.

Re, F., Cambianica, I., Sesana, S., Salvati, E., Cagnotto, A., Salmona, M., … Sancini, G. (2011). Functionalization with ApoE-derived peptides enhances the interaction with brain capillary endothelial cells of nanoliposomes binding amyloid-beta peptide. Journal of Biotechnology, 156(4), 341–346.

Reiss, Y., Hoch, G., Deutsch, U., & Engelhardt, B. (1998). T cell interaction with ICAM-1-deficient endothelium in vitro: Essential role for ICAM-1 and ICAM-2 in transendothelial migration of T cells. European Journal of Immunology, 28(10), 3086–3099.

Ronco, V., Potenza, D. M., Denti, F., Vullo, S., Gagliano, G., Tognolina, M., … Moccia, F. (2015). A novel Ca(2)(+)-mediated cross-talk between endoplasmic reticulum and acidic organelles: Implications for NAADPdependent Ca(2)(+) signalling. Cell Calcium, 57(2), 89–100.

Salvati, E., Re, F., Sesana, S., Cambianica, I., Sancini, G., Masserini, M., & Gregori, M. (2013). Liposomes functionalized to overcome the bloodbrain barrier and to target amyloid-beta peptide: The chemical design affects the permeability across an in vitro model. International Journal of Nanomedicine, 8, 1749–1758.

Sandow, S. L., Senadheera, S., Grayson, T. H., Welsh, D. G., & Murphy, T. V. (2012). Calcium and endothelium-mediated vasodilator signaling.
Advances in Experimental Medicine and Biology, 740, 811–831.

Sbano, L., Bonora, M., Marchi, S., Baldassari, F., Medina, D. L., Ballabio, A., … Pinton, P. (2017). TFEB-mediated increase in peripheral lysosomes regulates store-operated calcium entry. Scientific Reports, 7, 40797.

Scharbrodt, W., Abdallah, Y., Kasseckert, S. A., Gligorievski, D., Piper, H. M., Böker, D. K., … Oertel, M. F. (2009). Cytosolic Ca2+ oscillations in human cerebrovascular endothelial cells after subarachnoid hemorrhage. Journal of Cerebral Blood Flow and Metabolism, 29(1), 57–65.

Sharp, C. D., Hines, I., Houghton, J., Warren, A., Jackson, T. H., Jawahar, A., … Alexander, J. S. (2003). Glutamate causes a loss in human cerebral endothelial barrier integrity through activation of NMDA receptor. American Journal of Physiology: Heart and Circulatory Physiology, 285(6), H2592–H2598.

Shi, Y., Liu, X., Gebremedhin, D., Falck, J. R., Harder, D. R., & Koehler, R. C. (2008). Interaction of mechanisms involving epoxyeicosatrienoic acids, adenosine receptors, and metabotropic glutamate receptors in neurovascular coupling in rat whisker barrel cortex. Journal of Cerebral Blood Flow and Metabolism, 28(1), 111–125.

Siragusa, M., & Fleming, I. (2016). The eNOS signalosome and its link to endothelial dysfunction. Pflugers Archiv. European Journal of Physiology, 468(7), 1125–1137.

Smedler, E., & Uhlén, P. (2014). Frequency decoding of calcium oscillations. Biochimica et Biophysica Acta/General Subjects, 1840(3), 964–969.

Sonkusare, S. K., Bonev, A. D., Ledoux, J., Liedtke, W., Kotlikoff, M. I., Heppner, T. J., … Nelson, M. T. (2012). Elementary Ca2+ signals through endothelial TRPV4 channels regulate vascular function. Science, 336(6081), 597–601.

Stobart, J. L. L., Lu, L., Anderson, H. D. I., Mori, H., & Anderson, C. M. (2013). Astrocyte-induced cortical vasodilation is mediated by D-serine and endothelial nitric oxide synthase. Proceedings of the National Academy of Sciences of the United States of America, 110(8), 3149–3154.

Sun, W., McConnell, E., Pare, J. F., Xu, Q., Chen, M., Peng, W., … Nedergaard, M. (2013). Glutamate-dependent neuroglial calcium signaling differs between young and adult brain. Science, 339(6116), 197–200.

Sundivakkam, P. C., Natarajan, V., Malik, A. B., & Tiruppathi, C. (2013). Store-operated Ca2+ entry (SOCE) induced by protease-activated receptor-1 mediates STIM1 protein phosphorylation to inhibit SOCE in endothelial cells through AMP-activated protein kinase and p38beta mitogen-activated protein kinase. Journal of Biological Chemistry, 288(23), 17030–17041.

Syyong, H., Yang, H., Trinh, G., Cheung, C., Kuo, K., & van Breemen, C. (2009). Mechanism of asynchronous Ca(2+) waves underlying agonistinduced contraction in the rat basilar artery. British Journal of Pharmacology, 156(4), 587–600.

Sánchez-Hernández, Y., Laforenza, U., Bonetti, E., Fontana, J., Dragoni, S., Russo, M., … Moccia, F. (2010). Store-operated Ca(2+) entry is expressed in human endothelial progenitor cells. Stem Cells and Development, 19(12), 1967–1981.

Wen, Y., Li, J., Koo, J., Shin, S. S., Lin, Y., Jeong, B. S., … Goydos, J. S. (2014). Activation of the glutamate receptor GRM1 enhances angiogenic signaling to drive melanoma progression. Cancer Research, 74(9), 2499–2509.

Zhao, Z., Walczysko, P., & Zhao, M. (2008). Intracellular Ca2+ stores are essential for injury induced Ca2+ signaling and re-endothelialization. Journal of Cellular Physiology, 214(3), 595–603.

Zonta, M., Angulo, M. C., Gobbo, S., Rosengarten, B., Hossmann, K. A., Pozzan, T., & Carmignoto, G. (2003). Neuron-to-astrocyte signaling is central to the dynamic control of brain microcirculation. Nature Neuroscience, 6(1), 43–50.

Zuccolo, E., Bottino, C., Diofano, F., Poletto, V., Codazzi, A. C., Mannarino, S., … Moccia, F. (2016). Constitutive store-operated Ca(2+) entry leads to enhanced nitric oxide production and proliferation in infantile hemangioma-derived endothelial colony-forming cells. Stem Cells and Development, 25(4), 301–319.

Zuccolo, E., Dragoni, S., Poletto, V., Catarsi, P., Guido, D., Rappa, A., … Moccia, F. (2016). Arachidonic acid-evoked Ca2+ signals promote nitric oxide release and proliferation in human endothelial colony forming cells. Vascular Pharmacology, 87, 159–171.

Zuccolo, E., Lim, D., Kheder, D. A., Perna, A., Catarsi, P., Botta, L., … Moccia, F. (2017). Acetylcholine induces intracellular Ca2+ oscillations and nitric oxide release in mouse brain endothelial cells. Cell Calcium, 66, 33–47.

Zuccolo, E., Negri, S., Pellavio, G., Scarpellino, G., Laforenza, U., Sancini, G., … Moccia, F. (2018). Acetylcholine induces Ca2+ signals and nitric oxide release from human brain microvascular endothelial cells. Vascular Pharmacology, 103-105, 65.
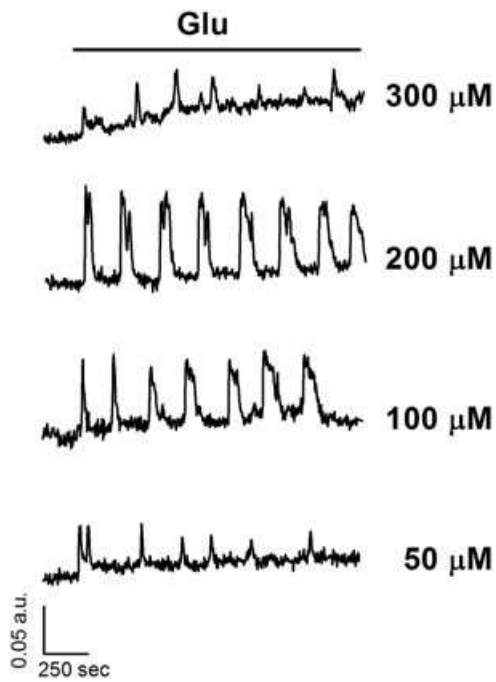
FIGURE 1   Glutamate evokes intracellular Ca^{2+} oscillations in bEND5 cells. Glutamate (Glu)-induced repetitive Ca^{2+} transients recorded at increasing concentrations in bEND5 cells. In this and the following figures, glutamate was added at the time indicated by the horizontal bar drawn around the Ca^{2+} tracings. The baseline of Ca^{2+} tracings has been shifted to avoid their overlapping for representation purposes
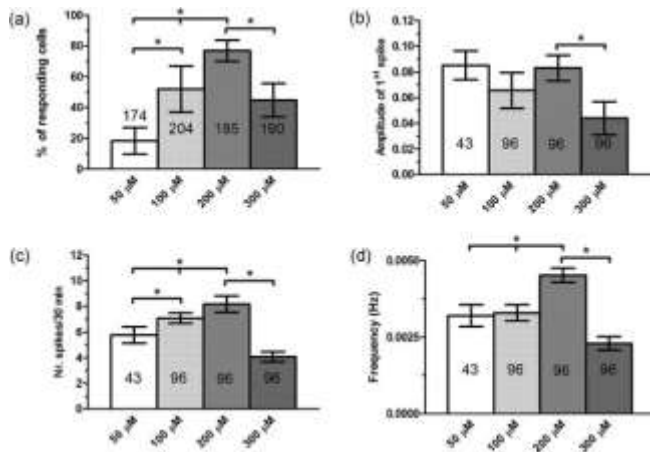
FIGURE 2 Statistical analysis of glutamate-induced intracellular Ca^{2+} oscillations in bEND5 cells. Bar histograms show the average ± SE of the percentage of responding cells (a), amplitude of the first spike (b), number of oscillations/30 min (c), and frequency (d) of glutamate-evoked intracellular Ca^{2+} oscillations. The asterisk indicates $p < 0.05$. SE: standard error
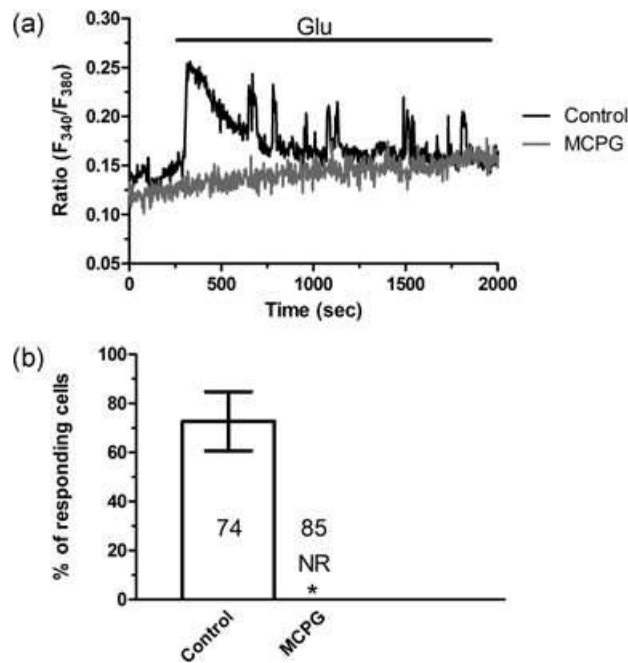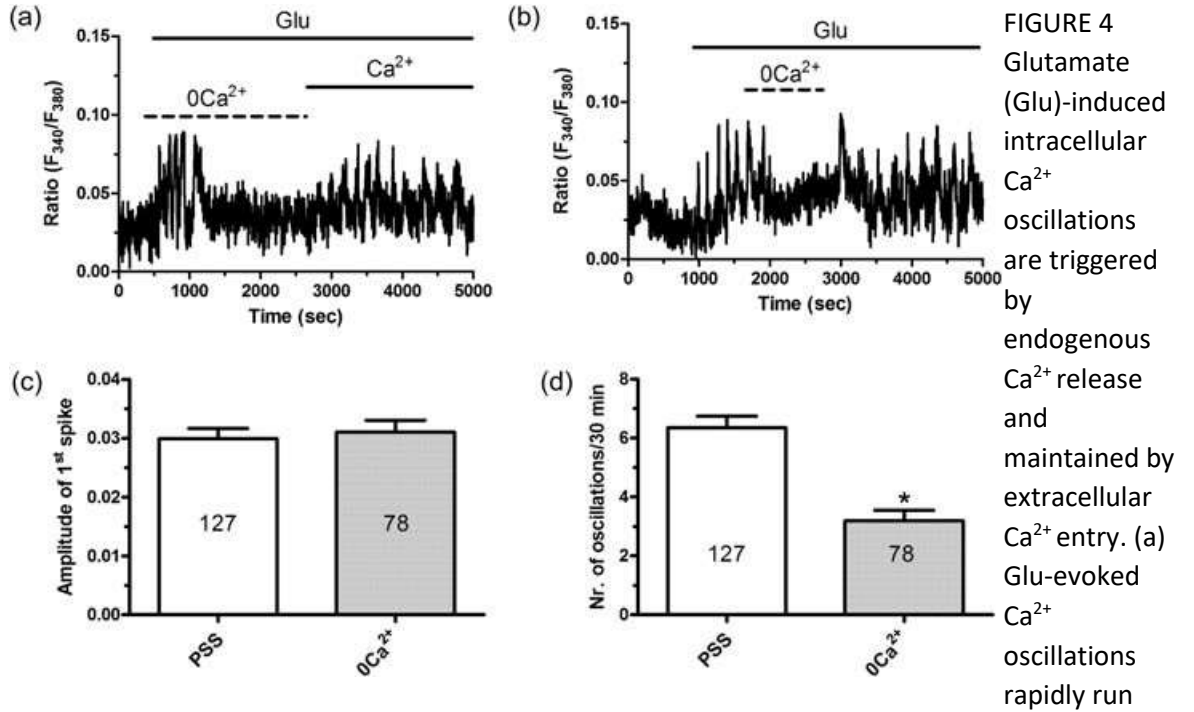

FIGURE 3 The pharmacological blockade of metabotropic glutamate receptors suppresses glutamate-induced intracellular Ca^{2+} oscillations. (a) Removal of glutamate (Glu) from the extracellular solution caused the reversible interruption of the ongoing Ca^{2+} spikes. (b) MCPG (150 µM, 10 min) suppressed the Ca^{2+} response to glutamate (200 µM). (c) Average ± SE of the percentage of responding cells in the absence and presence of MCPG.

The asterisk indicates $p < 0.05$. MCPG: α-methyl-4-carboxyphenylglycine; SE: standard error

FIGURE 4 Glutamate (Glu)-induced intracellular Ca^{2+} oscillations are triggered by endogenous Ca^{2+} release and maintained by extracellular Ca^{2+} entry. (a) Glu-evoked Ca^{2+} oscillations rapidly run down in the absence of external Ca^{2+} ($0Ca^{2+}$) but quickly resumed on Ca^{2+} restitution to the perfusate. (b) Removal of extracellular Ca^{2+} ($0Ca^{2+}$) during an established response caused the reversible decline of $[Ca^{2+}]_i$ to the baseline after 1–2 Ca^{2+} transients. (c) Bar histogram shows the average ± SE of the amplitude of the first Ca^{2+} transient induced by glutamate in the presence and absence of extracellular Ca^{2+} ($0Ca^{2+}$). (d) Bar histogram shows the average ± SE of the number of oscillations/30 min induced by Glu in the presence and absence of extracellular Ca^{2+} ($0Ca^{2+}$). The asterisk indicates $p < 0.05$. SE: standard error
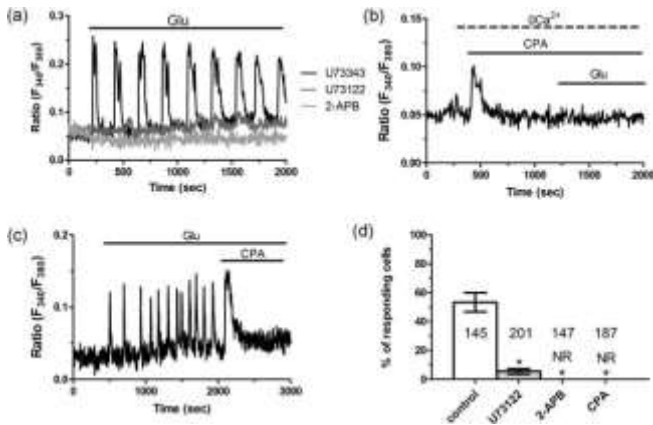
FIGURE 5 Repetitive Ca^{2+} release via InsP$_3$Rs support glutamate-induced intracellular Ca^{2+} oscillations. (a) Glutamate (Glu)-induced Ca^{2+} oscillations were inhibited by U73122 (10 µM, 30 min), an established PLC inhibitor, but not by structurally inactive analog, U73343 (10 µM; 30 min); moreover, Glu-evoked Ca^{2+} spikes were suppressed by 2-APB (50 µM, 30 min), which blocks InsP$_3$Rs. The baseline of Ca^{2+} tracings has been shifted to avoid their overlapping for representation purposes. (b) Depletion of the ER Ca^{2+} store with CPA (10 µM) under 0Ca^{2+} conditions caused a transient elevation in [Ca^{2+}]$_i$ and prevented the subsequent Ca^{2+} response to Glu. (c) Addition of CPA (10 µM) during Glu-induced intracellular Ca^{2+} oscillations caused an immediate increase in [Ca^{2+}]$_i$ because of passive depletion of the ER Ca^{2+} pool followed by blockade of ongoing oscillations. (d) Bar histogram shows the average ± SE of the percentage of responding cells under the designated treatments. The asterisk indicates p < 0.05. APB: aminoethoxydiphenylborate; CPA: cyclopiazonic acid; InsP3Rs: InsP3 receptors;
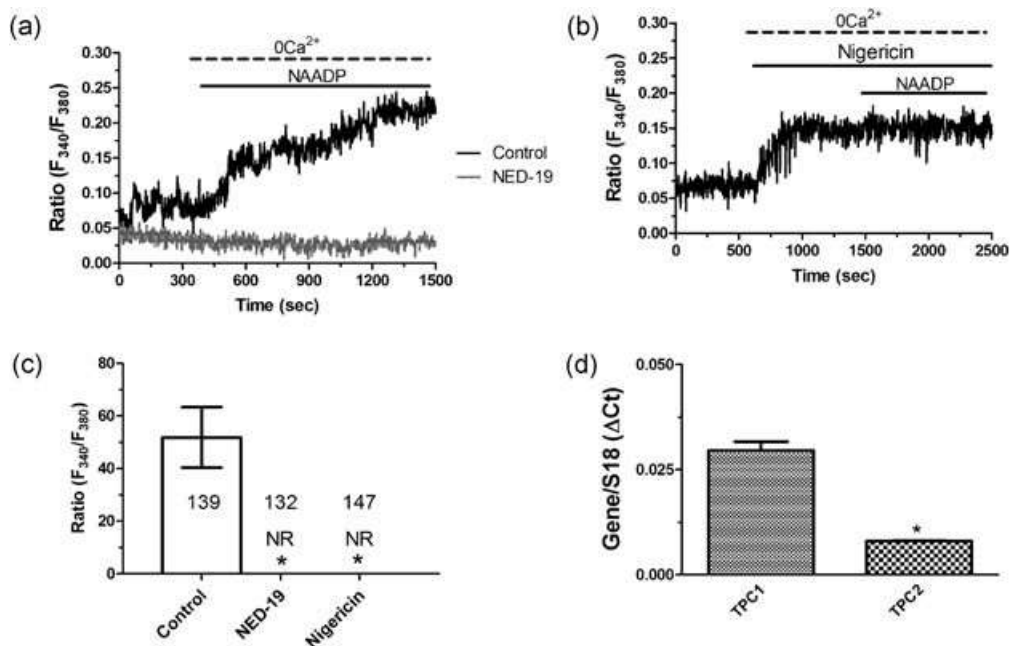
FIGURE 6 A functional endolysosomal Ca^{2+} store is present in bEND5 cells. (a) Liposomal delivery of NAADP induced a robust increase in $[Ca^{2+}]_i$ under $0Ca^{2+}$ conditions that was abrogated by NED-19 (10 µM, 30 min), which selectively blocks NAADP-induced Ca^{2+} release.

(b) Depleting the EL Ca^{2+} store with nigericin (50 µM, 20 min) prevented the Ca^{2+} response to NAADP. (c) Bar histogram shows the average ± SE of the magnitude of the NAADP-induced Ca^{2+} elevation under $0Ca^{2+}$ conditions in the absence and presence of NED-19. The asterisk indicates $p < 0.05$. (d) qRT-PCR analysis of TPCs revealed that TPC1 transcripts are more abundant as compared with those encoding for TPC2.

Data are expressed as average ± SE of qRT-PCR runs performed in triplicate. The asterisk indicates $p < 0.05$. EL: endolysosomal; NAADP: nicotinic acid adenine dinucleotide phosphate; qRT-PCR: quantitative real-time polymerase chain reaction; SE: standard error; TPC: two-pore
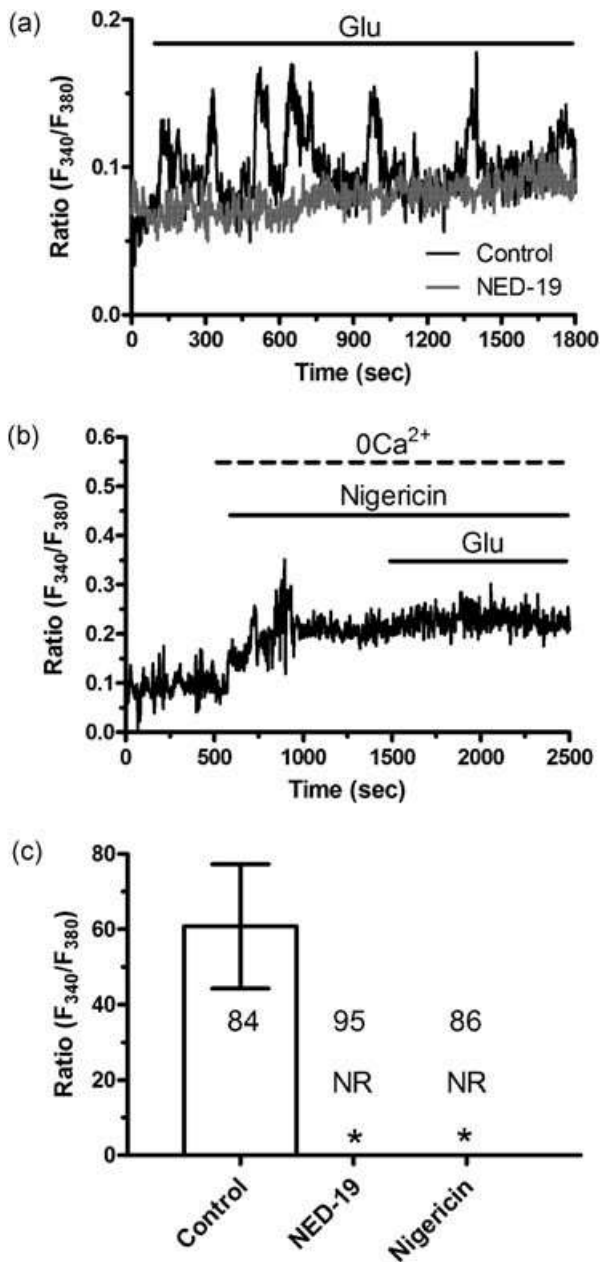
FIGURE 7 NAADP-induced Ca^{2+} release contributes to glutamate-induced intracellular Ca^{2+} oscillations. (a) Glutamate (Glu)-evoked Ca^{2+} oscillations were abrogated by NED-19 (10 μM, 30 min). (b) Glutamate (Glu)-evoked intracellular Ca^{2+} oscillations were suppressed on depletion of the EL Ca^{2+} store with nigericin (50 μM, 20 min). (c) Bar histogram shows the average ± SE of the percentage of responding cells under the designated treatments. The asterisk indicates $p < 0.05$. EL: endolysosomal; NAADP: nicotinic acid adenine dinucleotide phosphate; SE: standard error
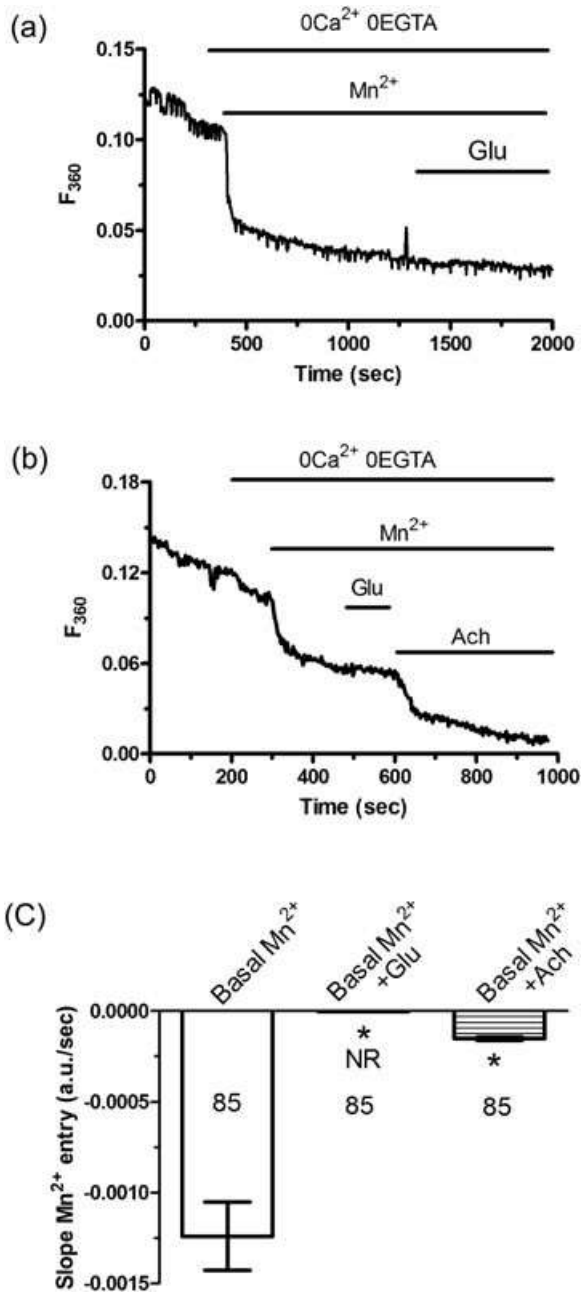
FIGURE 8 Constitutive SOCE maintains glutamate-induced intracellular Ca^{2+} oscillations in bEND5 cells. (a) Resting Ca^{2+} entry in mouse brain microvascular endothelial cells was evaluated by using the Mn^{2+}-quenching technique as described in Section 2. The extracellular PSS was first replaced with a $0Ca^{2+}$ solution, and then 200 μM Mn^{2+} was added to cause an immediate decay in Fura-2 fluorescence.
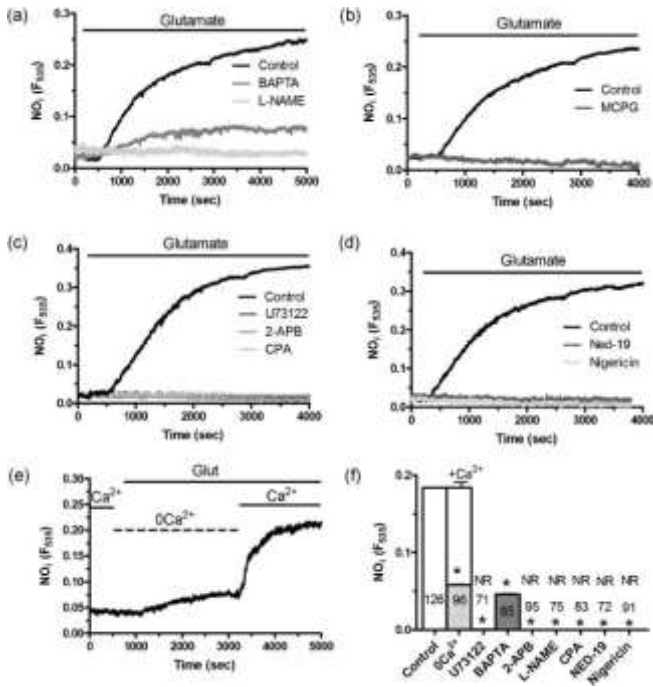
FIGURE 9 Glutamate-induced intracellular Ca^{2+} oscillations drive NO release in bEND5 cells. (a) In bEND5 cells loaded with the NO-sensitive fluorophore, DAF-FM, glutamate (Glu; 200 μM), caused a robust although delayed increase in NO-dependent signal, which was strongly reduced by either L-NAME (100 μM, 1 hr), a selective NOS blocker, or BAPTA (30 μM, 2 hr), a membrane-permeable intracellular Ca^{2+} chelator. (b) Glu-induced NO release was suppressed by MCPG (150 μM, 10 min), a selective antagonist of type I mGluRs. (c) Glu-induced NO release was unaffected by U73343 (10 μM; 30 min), whereas it was abolished by U73122 (10 μM, 30 min), 2-APB (50 μM, 30 min), and CPA (10 μM; 30 min). (c) Glu-induced NO production was inhibited by pretreating the cells with NED-19 (10 μM, 30 min) or nigericin (50 μM, 20 min). (e) Glu induced a sizeable, although reduced increase in NO levels under $0Ca^{2+}$ conditions, whereas NO release rapidly resumed on the restitution of extracellular Ca^{2+}. (f) average ± SE of the magnitude of Glu-induced NO synthesis under the designated treatments. The asterisk indicates $p < 0.05$. APB: aminoethoxydiphenylborate; BAPTA: 1,2-bis(o-aminophenoxy)ethane-N,N,N',N'-tetraacetic acid; CPA: cyclopiazonic acid; DAF-FM: 4-amino-5-methylamino-2',7'-difluorofluorescein; L-NAME: L-NG-Nitroarginine methyl ester; mGluR: metabotropic glutamate receptor; MCPG: α-methyl-4-carboxyphenylglycine; NO: nitric oxide; NOS: NO synthase; SE: standard error
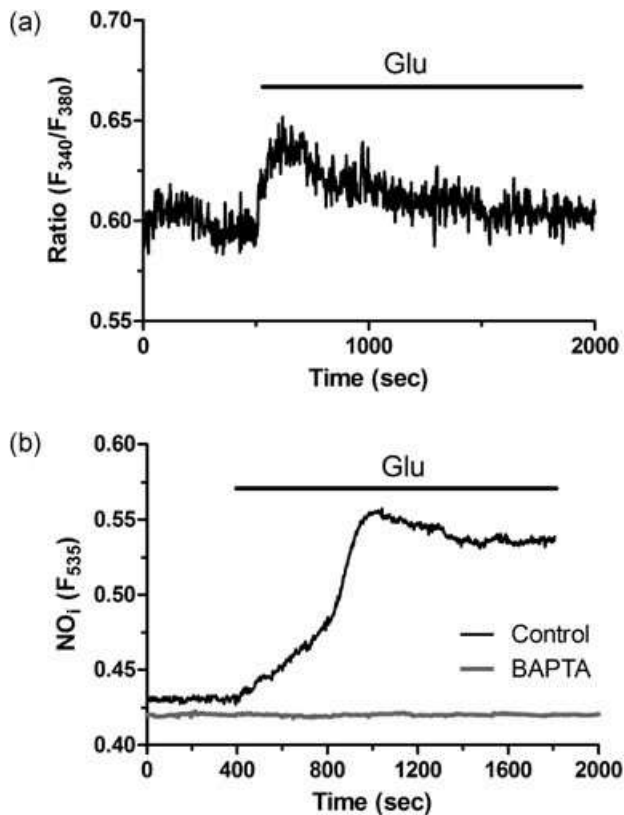
FIGURE 10 Glutamate evokes Ca^{2+}-dependent NO release in human microvascular brain endothelial cells. (a) Glutamate (Glu; 200 µM) caused an increase in $[Ca^{2+}]_i$ in hCMEC/D3 cells, an established model of human brain microvascular endothelial cells, loaded with Fura-2/AM. The trace is representative of 55 experiments. (b) Glu (200 µM) caused an immediate increase in DAF-FM fluorescence in hCMEC/D3 cells in the absence, but not in the presence, of BAPTA (30 µM, 2 hr). The NO traces are representative of 43 and 62 cells, respectively, from three separate experiments. BAPTA: 1,2-bis(o-aminophenoxy)ethane-N,N,N',N'-tetraacetic acid; DAF-FM: 4-amino-5-methylamino-2',7'-difluorofluorescein; NO: nitric oxide